Tangential Contact

4

4.1 Introduction

In this chapter, we will consider contacts which are loaded both in the normal direction z (as previously, z points into the half-space and $\tilde{z}$ to out of the half-space) and in the tangential direction x. Although the load now lacks rotational symmetry due to the bias for the x-direction, each of the non-vanishing components of stress tensor or displacement in the contact plane still have an approximately axisymmetric distribution. In this sense, this case can also be considered a rotationally symmetric contact problem.

Initially, we examine the deformation of an elastic half-space under the effect of a concentrated force at a point on the surface, which we define as the origin (Fig. 4.1).

Let the force $\underline{F}$ have a sole component in the x-direction. The components of the displacement vector $\underline{u} = (u, v, w)_{\{x,y,z\}}$ at the surface ($z = 0$) are given by the following (Cerruti 1882; Landau and Lifshitz 1991):

$$\begin{aligned} u &= F_x \frac{1}{4\pi G} \left\{ 2(1-\nu) + \frac{2\nu x^2}{r^2} \right\} \frac{1}{r}, \\ v &= F_x \frac{1}{4\pi G} \cdot \frac{2\nu}{r^3} xy, \\ w &= F_x \frac{1}{4\pi G} \cdot \frac{(1-2\nu)}{r^2} x, \end{aligned} \tag{4.1}$$

where G stands for the shear modulus. For a stress distribution with a sole stress component $\sigma_{xz}(x, y)$ acting in the surface, the displacements are determined using

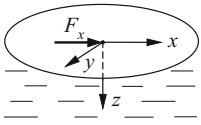

Fig. 4.1 Single tangential force acting on the surface of a half-space

V.L. Popov, M. Heß, E. Willert, *Handbook of Contact Mechanics*,
https://doi.org/10.1007/978-3-662-58709-6_4

the principle of superposition:

$$
\begin{aligned}
u(x,y) &= \frac{1}{4\pi G}\int\left\{2(1-\nu)+\frac{2\nu\,(x-x')^2}{r^2}\right\}\frac{1}{r}\sigma_{xz}(x',y')\mathrm{d}x'\mathrm{d}y',\\
v(x,y) &= \frac{2\nu}{4\pi G}\int\frac{1}{r^3}\left(x-x'\right)\left(y-y'\right)\sigma_{xz}(x',y')\mathrm{d}x'\mathrm{d}y',\\
w(x,y) &= \frac{(1-2\nu)}{4\pi G}\int\frac{1}{r^2}\left(x-x'\right)\sigma_{xz}(x',y')\mathrm{d}x'\mathrm{d}y',\\
r &= \sqrt{(x-x')^2+(y-y')^2}.
\end{aligned}
\tag{4.2}
$$

These equations lay the basis of all analytical and also numerical contact mechanical solutions and enable certain general deductions. For two contacting bodies under tangential load, the normal displacements of their surfaces are only then equal and opposite if the coefficients preceding the integral in the third equation of the set (4.2) are equal:

$$
\frac{1-2\nu_1}{G_1}=\frac{1-2\nu_2}{G_2}. \tag{4.3}
$$

The vertical displacements of both bodies are, in this case, "congruent", causing no additional interaction in the normal direction. We refer to these cases as decoupled normal and tangential contact problems. Bodies that meet condition (4.3) are called "elastically similar". This condition is met in two cases (among many others) of practical importance: (a) contact of bodies with the same elastic properties (e.g., wheel-rail contact), or (b) contact of a rigid body ($G_1 \to \infty$) with an incompressible one ($\nu_2 = 0.5$) (e.g., road-tire contact). If (4.3) is not fulfilled, the normal stresses then lead to relative tangential displacements of the contact partners and vice-versa. The mathematical treatment and the complete analytical solutions of the contact problems in particular are rendered far more difficult in this case. However, the solution differs only slightly from the case of elastically similar materials in many cases.

If the single stress component $\sigma_{xz}(x,y)$ is solely dependent on the polar radius r according to the law

$$
\sigma_{xz}(x,y)=\tau(x,y)=\tau_0(1-r^2/a^2)^{-1/2}, \tag{4.4}
$$

substituting into (4.2) with subsequent integration yields the result (Johnson 1985):

$$
u=\frac{\pi(2-\nu)}{4G}\tau_0 a=\text{const.} \tag{4.5}
$$

The tangential force is calculated to:

$$
F_x=\int_0^a\frac{2\pi r\,\tau_0\mathrm{d}r}{(1-r^2/a^2)^{1/2}}=2\pi a^2\tau_0. \tag{4.6}
$$

The physical implementation of the stress distribution (4.4) is more complicated than is the case for the analogous normal stress distribution. One might assume it could be achieved by tangentially displacing (4.5) a rigid punch of the radius a. However, this is only true if the resulting normal displacements also vanish. In the case of a rigid indenter, this condition is only fulfilled if the elastic half-space is incompressible. A constant displacement of the contact area is also achieved when two elastically similar half-spaces, stuck together in a circular area of radius a, are displaced relative to one another. The relative displacement of the bodies is then given by the superposition of the displacements of the form (4.5) for both bodies:

$$u^{(2)} - u^{(1)} = \pi \tau_0 a \left(\frac{2-\nu_1}{4G_1} + \frac{2-\nu_2}{4G_2} \right). \tag{4.7}$$

From this, accounting (4.6) we obtain the relationship:

$$F_x = 2G^* a (u^{(2)} - u^{(1)}), \tag{4.8}$$

with

$$\frac{1}{G^*} = \frac{2-\nu_1}{4G_1} + \frac{2-\nu_2}{4G_2}. \tag{4.9}$$

The coefficient connecting the force and the relative displacement (4.8) is the tangential contact stiffness:

$$k_x = 2G^* a. \tag{4.10}$$

Generally, when two bodies with curved surfaces are brought into normal contact and subsequently displaced in a tangential direction relative to one another, the bodies remain stuck to each other in one part of the contact area while in other areas slipping relative to one another. This is already indicated by the fact that the normal pressure vanishes at the boundary, while the tangential stress (4.4) at the boundary of a no-slip contact is singular. Therefore, the no-slip condition for a finite coefficient of friction can generally not be fulfilled in the vicinity of the contact boundary. Cattaneo (1938) and Mindlin (1949) independently solved the associated contact problem with some simplifying assumptions. These assumptions are:

- The existence of a single tangential stress component $\sigma_{xz}(r)$ in the slip plane, which only depends on the polar radius r.
- A unilateral displacement field with a displacement component only in the x-direction.
- Satisfaction of the following boundary conditions:
  - Equal displacements of both bodies in the stick zone, i.e., under the condition that the tangential stress is lower than μ times the normal stress:

$$u^{(1)}(r) = u^{(2)}(r), \quad \text{if } |\sigma_{xz}(r)| \leq \mu p(r) \quad \text{(stick)}. \tag{4.11}$$

– Local compliance with Coulomb's law of friction in the slip zone.

$$\sigma_{xz}(r) = -\mu p(r)\,\mathrm{sgn}(\dot{u}_1 - \dot{u}_2), \quad \text{otherwise (slip)}. \tag{4.12}$$

Axially symmetric contacts only approximately satisfy these conditions. A stress component $\sigma_{xz}(r)$ depending on r causes displacements in both x-direction and y-direction. The displacements and the friction forces are therefore not anti-parallel, thus violating the isotropic nature of Coulomb's law of friction. Johnson (1955) was the first to point out this error in the Cattaneo–Mindlin solution. He demonstrated that the maximum deviation of the directions of the displacement and friction force is on the order of $\nu/(4-\nu)$, and therefore lies between 0.09 for $\nu = 1/3$ and 0.14 for $\nu = 1/2$. Based on this finding, Johnson concluded that the Cattaneo–Mindlin solution provides a good approximation. Indeed, in macroscopic relationships (e.g., dependency of the tangential force on the tangential displacement) it results in an error in the order of 1%. However, local deviations (potentially important for wear, for example) may be significantly higher.

In this book we will examine tangential contacts in Cattaneo–Mindlin approximation, referring to these as "*Cattaneo–Mindlin problems*".

4.2 Cattaneo–Mindlin Problems

In the Cattaneo–Mindlin approximation, the tangential contact problem between two elastic bodies can be reduced to the contact problem of a rigid punch and an elastic half-space. Formulation of the equivalent problem of a rigid indenter and an elastic half-space requires using the previously introduced effective moduli E^* (see (2.1)) and G^* (see (4.9)), which we will list once more in this chapter as follows:

$$\begin{aligned} \frac{1}{E^*} &= \frac{1-\nu_1}{2G_1} + \frac{1-\nu_2}{2G_2}, \\ \frac{1}{G^*} &= \frac{2-\nu_1}{4G_1} + \frac{2-\nu_2}{4G_2}. \end{aligned} \tag{4.13}$$

These effective moduli uniquely define the contact properties of arbitrarily shaped bodies. For flat cylindrical punches of radius a, they directly define the normal and tangential stiffness of the contact (under the assumption of complete stick), as demonstrated in (2.21) and (4.10):

$$\begin{aligned} k_z &= 2E^*a, \\ k_x &= 2G^*a. \end{aligned} \tag{4.14}$$

We will assume that the simplest, local form of Coulomb's law of friction is valid in the contact area, which is given by (4.11) and (4.12). As mentioned in the introduction, small displacements in the y-direction also exist. These will be neglected here; the interested reader can be referred to the works of Vermeulen and Johnson (1964).

In contrast to the normal contact problem, tangential contacts exhibit *hysteresis* and *memory* properties. These properties mean that there is no universal relationship between the tangential force and the tangential displacement. Generally, at least part of the contact area in tangentially loaded contacts is a zone of local slip. The resulting energy dissipation causes hysteresis loops between the global contact quantities: force and displacement. Moreover, the tangentially loaded contact saves a part of its loading history in the form of tangential stresses; in this sense the contact can be said to possess a memory. However, this means that the state expressed by the stresses and displacements, depends on the entire previous loading history, at least for the tangential stresses and displacements. This dependency distinguishes the problems examined in this chapter from the previously discussed purely normal contacts, where the entire current contact configuration is defined by the current value of a single relevant contact quantity, e.g., the indentation depth. Therefore, the consideration of the tangential contact problem theoretically includes not only the specification of the indenter geometry and material properties, but also the complete loading or displacement history. For the sake of brevity in this chapter, we will restrict our consideration to the simplest and most technically relevant loading history, which consists of a constant normal force F_N and a subsequent application of an increasing tangential force F_x. For the consideration of more general loading histories, the reader can be referred to the pioneering publication by Mindlin and Deresiewicz (1953) and to work by Jäger (1993).

Let us consider the indentation of a rigid profile in an elastic half-space with the effective elastic properties given by the effective moduli (4.13). We will use the notation F_N for the normal force and F_x for the tangential force, a for the contact radius, and d and $u^{(0)}$ for the displacement of the rigid indenter in the normal and tangential direction, respectively. As explained earlier in this chapter, the contact area is generally composed of an inner stick zone of radius $c \leq a$ and an outer slip zone at the boundary of the contact area. The mixed boundary conditions at the surface of the elastic half-space at $z = 0$ are then as follows:

$$\begin{aligned} w(r) &= d - f(r), & r \leq a, \\ u(r) &= u^{(0)}, & r \leq c, \\ \sigma_{xz}(r) &= \mu\sigma_{zz}(r), & c < r \leq a, \\ \sigma_{zz}(r) &= 0, & r > a, \\ \sigma_{xz}(r) &= 0, & r > a. \end{aligned} \tag{4.15}$$

Here w and u represent the displacement of the half-space in the z and x-direction. The radii of the contact area and stick zone are unknown *a priori* and must be determined as part of the solution process.

4.3 Solution of the Tangential Contact Problem by Reducing to the Normal Contact Problem

Using a principle discovered independently by Ciavarella (1998) and Jäger (1998), the solution for the contact problem described in (4.15) can be determined if the solution of the corresponding frictionless normal contact problem is known. Therefore, we can make use of the solutions of various Boussinesq problems from the first chapters during our consideration of the Cattaneo–Mindlin problem in relation to those same profile shapes.

Let $\sigma_{zz}(r;\tilde{a})$ be the stress distribution in a normal contact of contact radius $\tilde{a}$. And let $w(r;\tilde{a})$ be the normal displacement resulting from this stress distribution. Ciavarella (1998) and Jäger (1998) were able to prove that the distribution of tangential stresses in the form of

$$\sigma_{xz}(r) = \mu \begin{cases} \sigma_{zz}(r;a) - \sigma_{zz}(r;c), & r \le c, \\ \sigma_{zz}(r;a), & c < r \le a \end{cases} \tag{4.16}$$

with the radius of the stick zone from the equation

$$G^* |u^{(0)}| = \mu E^* [d(a) - d(c)] \tag{4.17}$$

satisfy the boundary conditions (4.15), and therefore represent the solution of the corresponding tangential contact problem. The relationship between the forces and the contact radii is obtained from integration of the tangential stresses:

$$F_x = \mu [F_N(a) - F_N(c)]. \tag{4.18}$$

From the superposition of the tangential stresses (4.16), it immediately follows that the principle of superposition equally applies to the tangential displacements in the direction of the tangential force. The unknown tangential displacements outside the stick zone are given by:

$$u(r) = \frac{\mu E^*}{G^*} \begin{cases} d(a) - f(r) - w(r;c), & c < r \le a, \\ w(r;a) - w(r;c), & r > a. \end{cases} \tag{4.19}$$

Equations (4.16), (4.17), (4.18), and (4.19) provide a complete solution of the tangential contact problem via reduction to the normal contact problem.

4.4 Solution of the Tangential Contact Problem Using the MDR

As an alternative to the solution via reduction to the normal contact problem (detailed earlier in this chapter), the tangential contact problem can be solved "directly" (i.e., without knowledge of the solution of the normal contact problem) using the

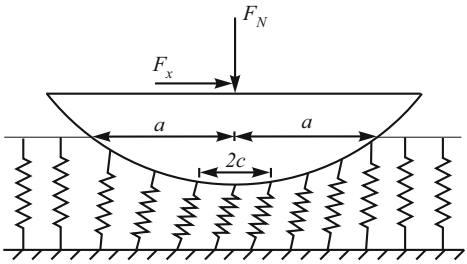

Fig. 4.2 Substitute model of the tangential contact

MDR (see Popov and Heß 2015). While ultimately the solutions do not differ for simple loading histories, this second approach can prove quite valuable for complex loading histories or numerical simulations.

Let us consider the axially symmetric indenter with the profile $\tilde{z} = f(r)$, which is initially pushed into the elastic half-space with the normal force F_N, and subsequently loaded with a tangential force F_x in x-direction. We will assume that the friction in the contact obeys Coulomb's law of friction in its simplest form, described by (4.11) and (4.12).

The application of a tangential force creates a ring-shaped slip zone, which expands inwards for an increasing force until complete slip sets in. We call the inner radius of the slip zone (also the radius of the stick zone) c.

In the MDR, this contact problem is solved as follows in this chapter (we will describe only the solution procedure. The complete derivation can be found in Chap. 11).

As in the case of the normal contact problem, we first determine the modified profile $g(x)$ using the transformation

$$g(x) = |x| \int_0^{|x|} \frac{f'(r)\mathrm{d}r}{\sqrt{x^2 - r^2}}. \tag{4.20}$$

Additionally, we define a Winkler foundation consisting of springs of normal and tangential stiffness

$$\begin{aligned} \Delta k_z &= E^* \Delta x, \\ \Delta k_x &= G^* \Delta x, \end{aligned} \tag{4.21}$$

where Δx is the distance between each spring and E^* and G^* are defined by (4.13). The calculation method involves indenting the Winkler foundation with the profile $g(x)$ under the normal force F_N, and subsequently tangentially displacing the profile by $u^{(0)}$ (see Fig. 4.2). The relationships between the indentation depth, the contact radius, and the normal force from the MDR model correspond exactly to the solution of the original problem, as explained in detail in Chap. 1 (while discussing the normal contact problem).

Each spring sticks to the indenting body and is displaced along with the body as long as the tangential force $\Delta F_x = \Delta k_x u^{(0)}$ of the particular spring is lower

than $\mu\Delta F_z$. Upon reaching the maximum static friction force, the spring begins to slip, with the force remaining constant and equal to $\mu\Delta F_z$. This rule can also be expressed in an incremental form for arbitrary loading histories: for small displacements $\Delta u^{(0)}$ of the indenter, the tangential displacements of the springs $u_{1D}(x)$ in the MDR model are given by:

$$\begin{aligned} \Delta u_{1D}(x) &= \Delta u^{(0)}, \quad \text{if } |\Delta k_x u_{1D}(x)| < \mu\Delta F_z, \\ u_{1D}(x) &= \pm\frac{\mu\Delta F_z(x)}{\Delta k_x}, \quad \text{in a state of slip.} \end{aligned} \tag{4.22}$$

The sign in the last equation depends on the direction of the tangential spring displacement, if the spring were sticking. By tracking the incremental difference of the indenter position we can uniquely determine the displacements of all springs in the contact area, thus yielding the values of all tangential forces:

$$\Delta F_x = \Delta k_x u_{1D}(x) = G^* \Delta x \cdot u_{1D}(x), \tag{4.23}$$

and the linear force density (distributed load):

$$q_x(x) = \frac{\Delta F_x}{\Delta x} = G^* u_{1D}(x). \tag{4.24}$$

The distribution of the tangential stress $\tau(r)$ and the displacements $u(r)$ in the original three-dimensional contact are defined by rules which are completely analogous to (2.13) and (2.14) of the normal contact problem:

$$\begin{aligned} \sigma_{xz} = \tau(r) &= -\frac{1}{\pi}\int_r^\infty \frac{q_x'(x)\mathrm{d}x}{\sqrt{x^2 - r^2}}, \\ u(r) &= \frac{2}{\pi}\int_0^r \frac{u_{1D}(x)\mathrm{d}x}{\sqrt{r^2 - x^2}}. \end{aligned} \tag{4.25}$$

Equations (4.22) to (4.25) are valid for arbitrary loading histories of the contact (and also for an arbitrary superposition of time-variant normal and tangential forces). In general, these equations must be implemented in a numerical program; this is extremely easy due to the independence of each spring in the Winkler foundation.

For simple loading conditions, the general solution can also be written in an explicit form. Let us illustrate the MDR procedure using the case of an indenter which is first pressed with an initial normal force F_N to generate a contact radius a, which is determined from the equation

$$\begin{aligned} F_N &= 2E^* \int_0^a w_{1D}(x)\mathrm{d}x = 2E^* \int_0^a [d - g(x)]\mathrm{d}x \\ &= 2E^* \int_0^a [g(a) - g(x)]\mathrm{d}x. \end{aligned} \tag{4.26}$$

Subsequently, the indenter is displaced in the tangential direction. The radius of the stick zone c is determined from the condition that the absolute tangential force is equal to the coefficient of friction μ multiplied with the normal force $\Delta k_z w_{1D}(c)$:

$$G^*|u^{(0)}| = \mu E^*[d - g(c)]. \tag{4.27}$$

From (4.27) we can draw an interesting and very general conclusion. The maximum tangential displacement for which the stick zone *just barely vanishes,* i.e., the minimum displacement to see complete slip, is determined by setting $c = 0$ in (4.27) (and therefore also $g(c) = 0$):

$$u_c^{(0)} = \mu \frac{E^*}{G^*} d. \tag{4.28}$$

Thus the displacement that is achieved before complete slip sets in is solely dependent on the indentation depth (and not on the shape of the indenter).

The tangential displacement in the MDR model at a given coordinate x then equals:

$$u_{1D}(x) = \begin{cases} u^{(0)}, & \text{for } x < c, \\ \mu \dfrac{E^*}{G^*}[d - g(x)], & \text{for } c < x < a, \\ 0, & \text{for } x > a, \end{cases} \tag{4.29}$$

and can also be written in the following simple universal form:

$$u_{1D}(x) = \mu \frac{E^*}{G^*}[w_{1D}(x;a) - w_{1D}(x;c)], \tag{4.30}$$

which corresponds to the principle of superposition by Ciavarella (1998) and Jäger (1998). The distributed load is obtained by multiplying with G^*:

$$q_x(x) = \begin{cases} G^* u^{(0)}, & \text{for } x < c, \\ \mu E^*[d - g(x)], & \text{for } c < x < a, \\ 0, & \text{for } x > a, \end{cases} \tag{4.31}$$

or

$$q_x(x) = \mu \left[q_z(x;a) - q_z(x;c)\right], \tag{4.32}$$

where $q_z(x;a)$ and $q_z(x;c)$ represent the respective distributed load of the normal contact problem with the radius a and c. The tangential force is given by:

$$F_x = 2 \int_0^a q_x(x) \mathrm{d}x = \mu[F_N(a) - F_N(c)], \tag{4.33}$$

where $F_N(a)$ and $F_N(c)$ mean the normal force with respect to the contact radii a or c. The stress distribution is obtained by substituting (4.31) into (4.25):

$$\tau(r) = \frac{\mu E^*}{\pi} \int_c^a \frac{g'(x)\mathrm{d}x}{\sqrt{x^2 - r^2}} = \mu[p(r;a) - p(r;c)]. \tag{4.34}$$

The displacements are calculated by inserting (4.29) into (4.25), resulting in:

$$u(r) = \frac{\mu E^*}{G^*}[w(r;a) - w(r;c)], \tag{4.35}$$

or explicitly:

$$u(r) = \begin{cases} u^{(0)}, & \text{for } r < c, \\ \dfrac{2}{\pi}\left[u^{(0)} \arcsin\left(\dfrac{c}{r}\right) + \dfrac{\mu E^*}{G^*}\displaystyle\int_c^r \frac{d - g(x)}{\sqrt{r^2 - x^2}}\mathrm{d}x\right], & \text{for } c < r < a, \\ \dfrac{2}{\pi}\left[u^{(0)} \arcsin\left(\dfrac{c}{r}\right) + \dfrac{\mu E^*}{G^*}\displaystyle\int_c^a \frac{d - g(x)}{\sqrt{r^2 - x^2}}\mathrm{d}x\right], & \text{for } r > a. \end{cases} \tag{4.36}$$

Equations (4.26)–(4.36) clearly show that this contact problem is completely defined when the shape of the indenter and one macroscopic quantity from each trio $\{d, a, F_N\}$ and $\{u^{(0)}, c, F_x\}$ are known. If the solution of the normal contact problem is known, all macroscopic quantities can be determined from (4.27) and (4.33). For the sake of simplicity and in analogy to Chap. 2, it is assumed that a and c are known quantities. Of course, this is not necessarily true. All other cases require rewriting the equations to solve for the unknown quantities. For instance, the relationship between the tangential force and the radius c of the stick zone is obtained by dividing (4.33) by F_N. Using partial integration, it can be rewritten in the compact form of:

$$\frac{F_x}{\mu F_N} = \frac{\int_c^a x g'(x)\mathrm{d}x}{\int_0^a x g'(x)\mathrm{d}x} = \frac{F_N(a) - F_N(c)}{F_N(a)}. \tag{4.37}$$

In summary, there are two approaches to solving the tangential contact problem for the simplest standard loading case (first normal and, subsequently, tangential):

I. The tangential contact problem is *reduced to the normal contact problem* using (4.33), (4.34), and (4.35) with the radius c of the stick zone being determined either by (4.27) (if the displacement is known) or (4.37) (if the force is known). For the sake of convenience, we will list all relevant equations once more:

$$
\begin{aligned}
F_x &= \mu[F_N(a) - F_N(c)], \\
\sigma_{xz}(r) &= \tau(r) = \mu[p(a) - p(c)], \\
u(r) &= \frac{\mu E^*}{G^*}[w(r;a) - w(r;c)], \quad \text{with } c \text{ from} \\
G^* u^{(0)} &= \mu E^* [d(a) - d(c)], \quad \text{or} \\
\frac{F_x}{\mu F_N} &= \frac{F_N(a) - F_N(c)}{F_N(a)}.
\end{aligned}
\tag{4.38}
$$

II. The tangential contact problem can also be solved directly, without knowledge of the corresponding solution of the normal contact problem, using (4.26), (4.27), (4.34), and (4.36), which we will also summarize once more:

$$
F_N = 2E^* \int_0^a [d - g(x)]\mathrm{d}x \quad \text{with } d = g(a),
$$

$$
F_x = 2\int_0^a q_x(x)\mathrm{d}x = 2\left(G^* u_x^{(0)} c + \mu E^* \int_c^a [d - g(x)]\,\mathrm{d}x\right),
$$

$$
\tau(r) = \frac{\mu E^*}{\pi} \int_c^a \frac{g'(x)\mathrm{d}x}{\sqrt{x^2 - r^2}},
$$

$$
u(r) = \begin{cases} u^{(0)}, & \text{for } r < c, \\ \dfrac{2}{\pi}\left[u^{(0)} \arcsin\left(\dfrac{c}{r}\right) + \dfrac{\mu E^*}{G^*}\displaystyle\int_c^r \frac{d - g(x)}{\sqrt{r^2 - x^2}}\mathrm{d}x\right], & \text{for } c < r < a, \\ \dfrac{2}{\pi}\left[u^{(0)} \arcsin\left(\dfrac{c}{r}\right) + \dfrac{\mu E^*}{G^*}\displaystyle\int_c^a \frac{d - g(x)}{\sqrt{r^2 - x^2}}\mathrm{d}x\right], & \text{for } r > a. \end{cases}
$$

Stick radius is determined by

$$
\begin{aligned}
G^* u^{(0)} &= \mu E^* [d - g(c)], \quad \text{or} \\
\frac{F_x}{\mu F_N} &= \frac{\int_c^a x g'(x)\mathrm{d}x}{\int_0^a x g'(x)\mathrm{d}x}.
\end{aligned}
\tag{4.39}
$$

If the stresses and displacements are known, the dissipated friction energy can also be calculated with

$$W_R = \int \Delta u \sigma_{xz} \mathrm{d}A. \tag{4.40}$$

Here, Δu represents the relative displacement between the indenter and the half-space. It vanishes in the stick zone. With the stresses outside of the contact also being zero, only the zone of local slip contributes to this integral. The integral can thus be reformulated to:

$$\begin{aligned} W_R(c,a) &= 2\pi\mu \int_c^a (u^{(0)} - u)\sigma_{zz} r \mathrm{d}r \\ &= \frac{2\pi\mu^2 E^*}{G^*} \int_c^a [f(r) + w(r;c) - d(c)]\sigma_{zz}(r;a) r \mathrm{d}r. \end{aligned} \tag{4.41}$$

However, it is easier to calculate the dissipated energy directly using the MDR model of the contact. Then we get:

$$\begin{aligned} W_R(c,a) &= -2G^* \int_c^a u_{1D} \Delta u_{1D} \mathrm{d}x \\ &= -2G^* \left(\frac{\mu E^*}{G^*} \right)^2 \int_c^a [d(a) - g(x)][g(x) - d(c)] \mathrm{d}x. \end{aligned} \tag{4.42}$$

Here, $d(a) = g(a)$ and $d(c) = g(c)$ are the indentation depths corresponding to the radii a and c.

Once again it should be noted that the detailed MDR algorithm is not restricted to the specifically examined loading case (application of a normal force with subsequent tangential loading). In the context of tangential problems, it is valid for all loading cases, including arbitrarily varying normal and tangential forces. Thus, we can utilize it for simulations of arbitrary loading histories, e.g., in stick-slip drives.

4.5 Areas of Application

The technical applications of mechanical contact problems with friction are virtually uncountable. Even by neglecting rolling contacts (not featured in this book due to their asymmetry) occurring in bearings or other types of transport elements, tangential contact problems are found in a wide range of applications, e.g., friction-based connections, friction-induced damping (such as in leaf springs), surface treatment via a sliding indenter (burnishing), or mechanical stick-slip linear drives which can be miniaturized to an extreme degree. In the latter two applications, the indenters usually appear in the classical shapes of the flat punch, cone, and sphere. Once

again we will consider these three bodies in their "pure form" (see Sects. 4.6.1, 4.6.2, and 4.6.3) as well as modifications thereof, owing to imperfections due to manufacturing or wear (see Sects. 4.6.5 to 4.6.10). As always, we will consider the profile in shape of a power-law (see Sect. 4.6.4), which is a basic building block of the solution in the form of a Taylor series of any sufficiently differentiable profile.

4.6 Explicit Solutions for Axially Symmetric Tangential Contact Problems

For the sake of simplicity, we will assume in the following that $u^{(0)} \geq 0$. This condition does not represent a restriction to the general validity of the presented results.

4.6.1 The Cylindrical Flat Punch

The solution of the normal contact problem for the indentation by a flat cylindrical punch of radius a according to Chap. 2 (see Sect. 2.5.1) is given by:

$$\begin{aligned} F_N(d) &= 2E^* d a, \\ \sigma_{zz}(r;d) &= -\frac{E^* d}{\pi\sqrt{a^2 - r^2}}, \quad r \leq a, \\ w(r;d) &= \frac{2d}{\pi} \arcsin\left(\frac{a}{r}\right), \quad r > a. \end{aligned} \tag{4.43}$$

Here, F_N represents the normal force, d the indentation depth, σ_{zz} the normal stress, and w the normal displacement of the half-space. Under tangential load, the contact is either sticking or slipping completely; there is no limited zone of local slip. The contact starts to slip once the tangential displacement of the punch reaches the critical value (4.28):

$$u_c^{(0)} = \frac{\mu E^*}{G^*} d. \tag{4.44}$$

The shear stress distribution in the contact equals

$$\sigma_{xz}(r;u^{(0)},d) = -\frac{G^*}{\pi\sqrt{a^2 - r^2}} \cdot \begin{cases} u^{(0)}, & \text{for } u^{(0)} \leq u_c^{(0)}, \\ u_c^{(0)}, & \text{for } u^{(0)} > u_c^{(0)} \end{cases} \tag{4.45}$$

and the tangential displacements outside the contact area $r > a$ are:

$$u(r;u^{(0)},d) = \frac{2}{\pi} \arcsin\left(\frac{a}{r}\right) \cdot \begin{cases} u^{(0)}, & \text{for } u^{(0)} < u_c^{(0)}, \\ u_c^{(0)}, & \text{for } u^{(0)} > u_c^{(0)}. \end{cases} \tag{4.46}$$

The total tangential force is:

$$F_x(u^{(0)}, d) = 2G^* a \cdot \begin{cases} u^{(0)}, & \text{for } u^{(0)} < u_c^{(0)}, \\ u_c^{(0)}, & \text{for } u^{(0)} > u_c^{(0)}. \end{cases} \tag{4.47}$$

4.6.2 The Cone

The consideration of the indentation by a cone with a slope angle θ in Chap. 2 (Sect. 2.5.2) in the context of frictionless normal contact yielded the following relationships for the indentation depth d, the contact radius a, the normal force F_N, the normal stresses σ_{zz}, and the normal displacements w:

$$\begin{aligned} d(a) &= \frac{\pi}{2} a \tan\theta, \\ F_N(a) &= \frac{\pi a^2}{2} E^* \tan\theta, \\ \sigma_{zz}(r;a) &= -\frac{E^* \tan\theta}{2} \operatorname{arcosh}\left(\frac{a}{r}\right), \quad r \le a, \\ w(r;a) &= \tan\theta \left(\sqrt{r^2 - a^2} - r + a \arcsin\left(\frac{a}{r}\right)\right), \quad r > a. \end{aligned} \tag{4.48}$$

The mean pressure in the contact area is:

$$p_0 = \frac{E^* \tan\theta}{2}. \tag{4.49}$$

The solution of the tangential contact problem depicted in Fig. 4.3 (which is the relationships between the tangential displacement $u^{(0)}$), the radius of the stick zone c, and the tangential force F_x (first published by Truman et al. 1995) is then expressed

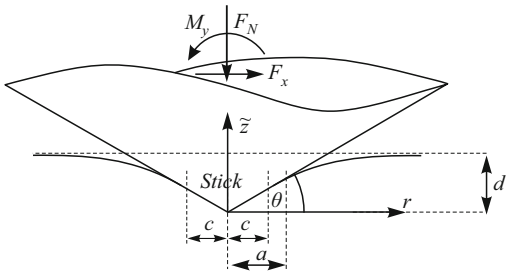

Fig. 4.3 Tangential contact of a rigid conical indenter and elastic half-space

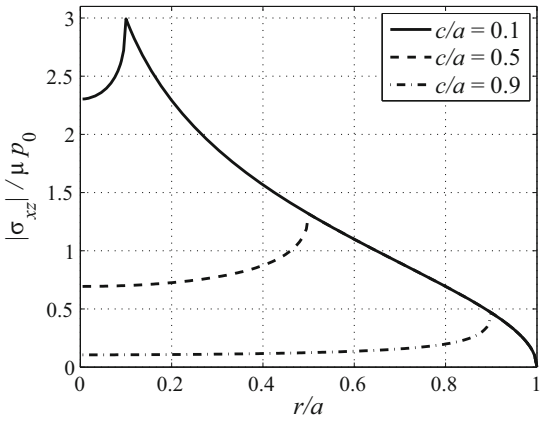

Fig. 4.4 Normalized tangential stresses in contact for different values of the normalized radius of the stick zone c/a when indented by a cone

by (4.38) as follows:

$$\begin{aligned} u^{(0)}(a,c) &= \frac{\pi\mu E^*}{2G^*}(a-c)\tan\theta, \\ u_c^{(0)}(a) &= \frac{\pi\mu E^*}{2G^*}a\tan\theta, \\ F_x(a,c) &= \frac{\mu\pi E^*\tan\theta}{2}(a^2-c^2) = \mu F_N(a)\left(1-\frac{c^2}{a^2}\right). \end{aligned} \tag{4.50}$$

For the missing tangential stresses and displacements one gets:

$$\begin{aligned} \sigma_{xz}(r;a,c) &= -\frac{\mu E^*\tan\theta}{2}\begin{cases} \operatorname{arcosh}\left(\frac{a}{r}\right)-\operatorname{arcosh}\left(\frac{c}{r}\right), & r\le c, \\ \operatorname{arcosh}\left(\frac{a}{r}\right), & c<r\le a, \end{cases} \\ u(r;a,c) &= \frac{\mu E^*\tan\theta}{G^*}\begin{cases} -c\arcsin\left(\frac{c}{r}\right)+\frac{\pi a}{2}-\sqrt{r^2-c^2}, & c<r\le a, \\ a\arcsin\left(\frac{a}{r}\right)+\sqrt{r^2-a^2} & \\ \quad -c\arcsin\left(\frac{c}{r}\right)-\sqrt{r^2-c^2}, & r>a. \end{cases} \end{aligned} \tag{4.51}$$

These are shown in normalized form in Figs. 4.4 and 4.5. The finite value of the tangential stress in the middle of the contact is:

$$\lim_{r\to 0}\left(\frac{|\sigma_{xz}|}{\mu p_0}\right) = \lim_{r\to 0}\left[\operatorname{arcosh}\left(\frac{a}{r}\right)-\operatorname{arcosh}\left(\frac{c}{r}\right)\right] = \ln\left(\frac{a}{c}\right). \tag{4.52}$$

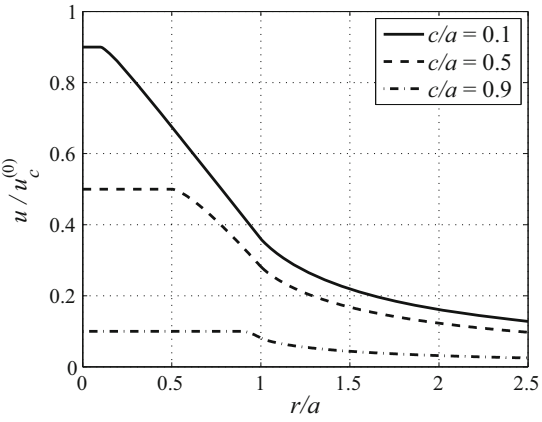

Fig. 4.5 Normalized tangential displacements of the half-space for different values of the normalized radius of the stick zone c/a when indented by a cone

The loss of mechanical energy is calculated according to (4.42):

$$W_R(a,c) = -\frac{(\pi\mu E^* \tan\theta)^2}{12G^*}(a-c)^3. \tag{4.53}$$

In normalized variables, this can be represented as:

$$\eta := \frac{|W_R|}{\mu F_N u_c^{(0)}} = \frac{1}{3}\left(1-\frac{c}{a}\right)^3. \tag{4.54}$$

4.6.3 The Paraboloid

As usual, the paraboloid was the first shape for which a broad class of contact problems was solved. In the case of the tangential contact, the classical solution goes back to Cattaneo (1938) and Mindlin (1949). The pure normal contact problem solution is represented by the following relationships linking indentation depth d, contact radius a, normal force F_N, normal stress σ_{zz}, and normal displacement w (see Sect. 2.5.3)

$$\begin{aligned}
d(a) &= \frac{a^2}{R},\\
F_N(a) &= \frac{4}{3}\frac{E^* a^3}{R},\\
\sigma_{zz}(r;a) &= -\frac{2E^*}{\pi R}\sqrt{a^2-r^2}, \quad r \le a,\\
w(r;a) &= \frac{a^2}{\pi R}\left[\left(2-\frac{r^2}{a^2}\right)\arcsin\left(\frac{a}{r}\right)+\frac{\sqrt{r^2-a^2}}{a}\right], \quad r > a.
\end{aligned} \tag{4.55}$$

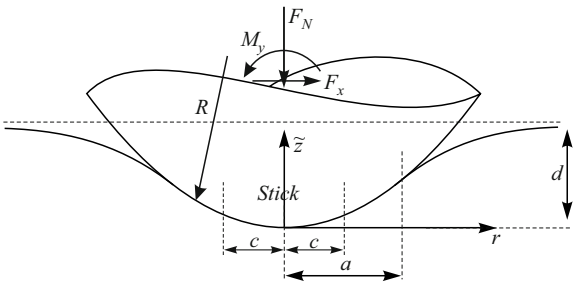

Fig. 4.6 Tangential contact of a rigid parabolic indenter and an elastic half-space

Here, R denotes the curvature radius of the paraboloid in the vicinity of the contact. The average pressure in the contact is:

$$p_0 = \frac{4E^* a}{3\pi R}. \tag{4.56}$$

Taking into account (4.38), the solution of the tangential problem (see Fig. 4.6) is given by the relationships

$$\begin{aligned} u^{(0)}(a,c) &= \frac{\mu E^*}{G^* R}(a^2 - c^2), \\ u_c^{(0)}(a) &= \frac{\mu E^*}{G^* R} a^2, \\ F_x(a,c) &= \frac{4\mu E^*}{3R}(a^3 - c^3) = \mu F_N(a)\left(1 - \frac{c^3}{a^3}\right), \end{aligned} \tag{4.57}$$

with the tangential displacement of the rigid paraboloid $u^{(0)}$, the radius c of the stick zone, and the tangential force F_x. The tangential stresses and displacements of the elastic half-space then amount to:

$$\sigma_{xz}(r;a,c) = -\frac{2\mu E^*}{\pi R}\begin{cases} \sqrt{a^2 - r^2} - \sqrt{c^2 - r^2}, & r \le c, \\ \sqrt{a^2 - r^2}, & c < r \le a, \end{cases}$$

$$u(r;a,c) = \frac{\mu E^*}{G^* R}\begin{cases} a^2 - \frac{r^2}{2} - \frac{c^2}{\pi}\left[\left(2 - \frac{r^2}{c^2}\right)\arcsin\left(\frac{c}{r}\right) + \frac{\sqrt{r^2 - c^2}}{c}\right], & c < r \le a, \\ \frac{a^2}{\pi}\left[\left(2 - \frac{r^2}{a^2}\right)\arcsin\left(\frac{a}{r}\right) + \frac{\sqrt{r^2 - a^2}}{a}\right] \\ \quad -\frac{c^2}{\pi}\left[\left(2 - \frac{r^2}{c^2}\right)\arcsin\left(\frac{c}{r}\right) + \frac{\sqrt{r^2 - c^2}}{c}\right], & r > a. \end{cases} \tag{4.58}$$

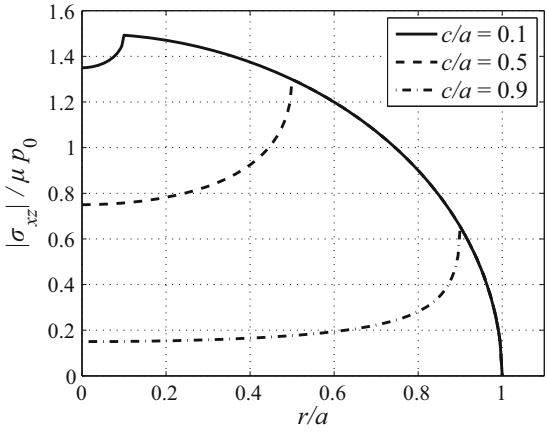

Fig. 4.7 Normalized tangential stresses in the contact for different values of the normalized stick zone radius c/a for indentation by a paraboloid

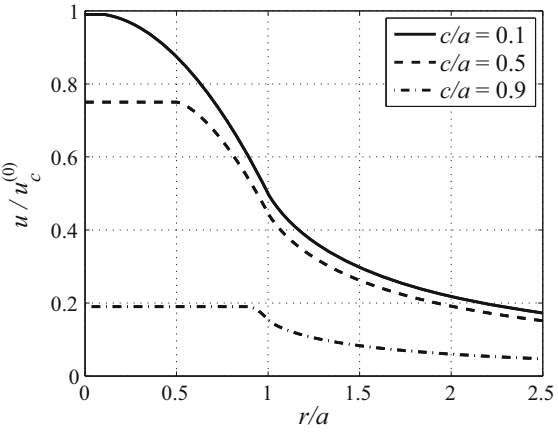

Fig. 4.8 Normalized tangential displacement of the half-space for different values of the normalized stick zone radius c/a for indentation by a paraboloid

These are visualized in normalized form in Figs. 4.7 and 4.8. Using (4.42), the loss of mechanical energy can be written as:

$$W_R(c,a) = -\frac{2(\mu E^*)^2}{G^* R^2} \int_c^a (a^2 - x^2)(x^2 - c^2)\mathrm{d}x. \tag{4.59}$$

When expressed in normalized quantities, it can be rewritten as:

$$\eta := \frac{|W_R|}{\mu F_N u_c^{(0)}} = \frac{1}{5}\left(1 - \frac{c}{a}\right)^3 \left(1 + 3\frac{c}{a} + \frac{c^2}{a^2}\right). \tag{4.60}$$

The Stresses in the Interior of the Half-Space

In the case of global slip, Hamilton and Goodman (1966) were able to determine the stresses in the interior of the half-space by introducing the complex functions

$$\begin{aligned} F &:= \frac{1}{2}(\tilde{z} - ia)R_2 + \frac{1}{2}r^2 \ln(R_2 + z_2), \\ G &:= -\frac{1}{3}R_2^3 + \frac{1}{2}\tilde{z}z_2R_2 - \frac{1}{3}ia^3 + \frac{1}{2}\tilde{z}r^2 \ln(R_2 + z_2), \\ H &:= \frac{4}{3}ia^3\tilde{z} - \frac{1}{6}\tilde{z}R_2^3 + \frac{1}{2}iaR_2^3 - \frac{1}{4}\tilde{z}r^2R_2 - \frac{1}{4}r^4 \ln(R_2 + z_2), \end{aligned} \tag{4.61}$$

with the imaginary unit i and the complex coordinates:

$$\begin{aligned} z_2 &:= \tilde{z} + ia, \\ R_2 &:= \sqrt{z_2^2 + r^2}. \end{aligned} \tag{4.62}$$

To avoid any misunderstandings, we will stress once more that $\tilde{z}$ represents the normal axis pointing out of the half-space while the z-axis points inwards. The stress configuration in the half-space is then defined by the imaginary parts of the expressions:

$$\begin{aligned} \hat{\sigma}_{xx} &:= -\frac{3}{2}\frac{\mu p_0}{a}\frac{x}{r^4}\left[\left(4\frac{x^2}{r^2} - 3\right)\left(H\nu - \frac{1}{2}\tilde{z}\frac{\partial H}{\partial \tilde{z}}\right) + y\frac{\partial H}{\partial y}\right. \\ &\qquad \left. + (1-\nu)\,x\frac{\partial H}{\partial x} + \frac{1}{2}x\tilde{z}\frac{\partial^2 H}{\partial x \partial \tilde{z}} - 2\nu r^2 F\right], \\ \hat{\sigma}_{yy} &:= -\frac{3}{2}\frac{\mu p_0}{a}\frac{x}{r^4}\left[\left(4\frac{y^2}{r^2} - 1\right)\left(H\nu - \frac{1}{2}\tilde{z}\frac{\partial H}{\partial \tilde{z}}\right) - \nu y\frac{\partial H}{\partial y}\right. \\ &\qquad \left. + \frac{1}{2}y\tilde{z}\frac{\partial^2 H}{\partial y \partial \tilde{z}} - 2\nu r^2 F\right], \\ \hat{\sigma}_{zz} &:= -\frac{3}{2}\frac{\mu p_0}{a}\frac{x\tilde{z}}{r^2}\frac{\partial F}{\partial \tilde{z}}, \\ \hat{\sigma}_{yz} &:= -\frac{3}{2}\frac{\mu p_0}{a}\frac{xy\tilde{z}}{2r^4}\frac{\partial^2 H}{\partial \tilde{z}^2}, \\ \hat{\sigma}_{xz} &:= -\frac{3}{2}\frac{\mu p_0}{a}\frac{1}{r^2}\left[2G + \frac{1}{2}\frac{\partial H}{\partial \tilde{z}} + \tilde{z}\frac{\partial}{\partial x}(xF) - 2\frac{\tilde{z}x^2}{r^2}F\right], \\ \hat{\sigma}_{xy} &:= -\frac{3}{2}\frac{\mu p_0}{a}\frac{y}{r^4}\left[\left(4\frac{x^2}{r^2} - 1\right)\left(H\nu - \frac{1}{2}\tilde{z}\frac{\partial H}{\partial \tilde{z}}\right) + \frac{1}{2}y\frac{\partial H}{\partial y}\right. \\ &\qquad \left. + \frac{1}{2}x(1-2\nu)\frac{\partial H}{\partial x} + \frac{1}{2}x\tilde{z}\frac{\partial^2 H}{\partial x \partial \tilde{z}}\right]. \end{aligned} \tag{4.63}$$

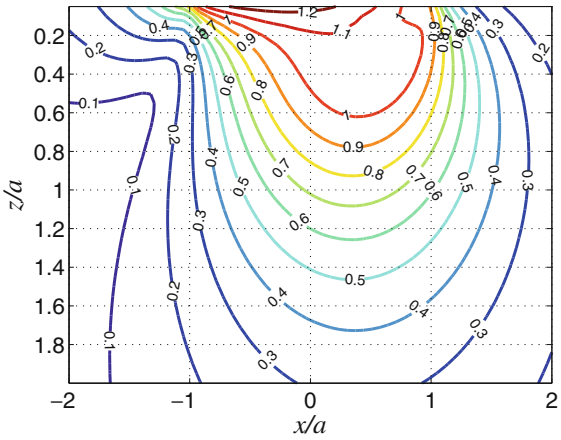

Fig. 4.9 Curve of the equivalent stress according to the von Mises criterion in the x–z-plane under a fully sliding tangential contact with a paraboloid, normalized to the average pressure in the contact

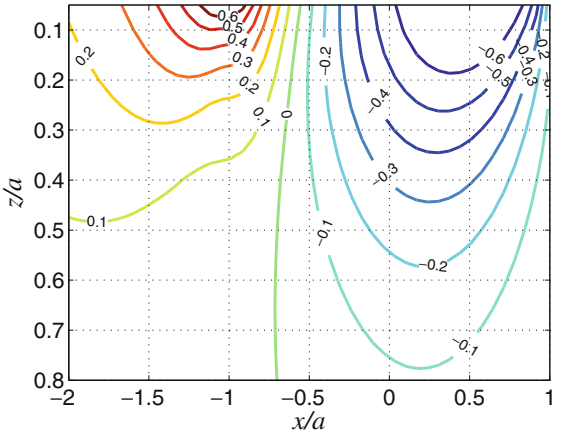

Fig. 4.10 Curve of the greatest principal stress in the x–z-plane under a fully slipping tangential contact with a paraboloid, normalized to the average pressure in the contact

To illustrate these expressions, consider Figs. 4.9 and 4.10. Depicted are the stress curves in the x–z-plane (i.e., the plane of the greatest stresses) of the equivalent stress, according to the von Mises criterion, and the greatest principal stress for a globally sliding contact with $\nu = 0.3$ and $\mu = 0.5$, both normalized to the average pressure in the contact. It is apparent that the leading edge of the contact experiences pressure while the trailing edge is under tension.

It can also be seen that the maximum of the equivalent stress has moved to the surface of the medium. This means that, in this case, the plastic deformation will begin at the surface of the elastic half-space. Since the maximum of the equivalent stress in the case of Hertzian (frictionless) contact lies underneath the surface (detailed in Sect. 2.5.3), there must exist a critical coefficient of friction for which this maximum reaches the surface. This value is of great technical significance for burnishing, a surface treatment which relies on the plastic deformation generated by the global sliding of the indenter. To achieve the desired property change using this

process, it is imperative that the equivalent stress maximum is located at the surface level. In the case of the contact of a parabolic indenter with a half-space, Johnson (1985) provided the limit of this coefficient of friction at $\mu_c = 0.3$.

4.6.4 The Profile in the Form of a Power-Law

In Chap. 2 (Sect. 2.5.8) the solution of the normal contact problem for an indenter with a general profile in the form of a power-law:

$$f(r) = br^n, \quad n \in \mathbb{R}^+, \tag{4.64}$$

with a positive real number n, has been derived. In order to not confuse the second constant in this function with the radius of the stick zone c, we call it b (in contrast to what it was called in previous chapters). When considering the normal contact, we found the following expressions ((2.63)–(2.65)):

$$\begin{aligned}
d(a) &= \kappa(n) b a^n, \\
F_N(a) &= E^* \frac{2n}{n+1} \kappa(n) b a^{n+1}, \\
\sigma_{zz}(r;a) &= -\frac{E^*}{\pi} n \kappa(n) b \int_r^a x^{n-1} \frac{\mathrm{d}x}{\sqrt{x^2 - r^2}}, \quad r \le a, \\
w(r;a) &= \frac{2}{\pi} \kappa(n) b \left[a^n \arcsin\left(\frac{a}{r}\right) - \int_0^a x^n \frac{\mathrm{d}x}{\sqrt{r^2 - x^2}} \right], \quad r > a,
\end{aligned} \tag{4.65}$$

for the indentation depth d, the contact radius a, the normal force F_N and the normal stresses σ_{zz}, and the normal displacements w of the half-space. Here, the stretch factor $\kappa(n)$ is defined as:

$$\kappa(n) := \sqrt{\pi} \frac{\Gamma(n/2+1)}{\Gamma[(n+1)/2]}, \tag{4.66}$$

with the gamma function $\Gamma(\cdot)$:

$$\Gamma(z) := \int_0^\infty t^{z-1} \exp(-t) \mathrm{d}t. \tag{4.67}$$

The solution of the tangential contact problem shown in Fig. 4.11 can be obtained using (4.38); that yields to the following relationships between global contact vari-

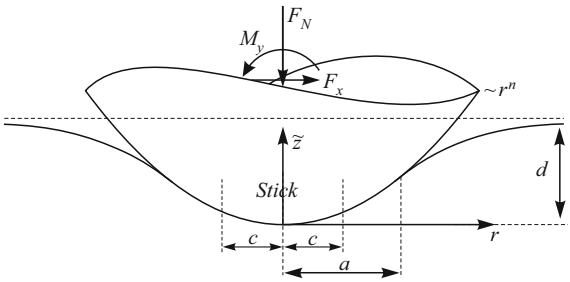

Fig. 4.11 Tangential contact between a rigid indenter with a profile in the form of a power-law and an elastic half-space

ables (displacement $u^{(0)}$ and tangential force F_x):

$$u^{(0)}(a,c) = \frac{\mu E^*}{G^*}\kappa(n)b(a^n - c^n),$$
$$u_c^{(0)}(a) = \frac{\mu E^*}{G^*}\kappa(n)ba^n,$$
$$F_x(a,c) = \mu E^* \frac{2n}{n+1}\kappa(n)b(a^{n+1} - c^{n+1}) = \mu F_N(a)\left(1 - \frac{c^{n+1}}{a^{n+1}}\right). \quad (4.68)$$

The tangential stresses and displacements can also be obtained by (4.38) using (4.65). The explicit representation is extensive, and should therefore be omitted here. For the treatment of integrals occurring in σ_{zz} and w—and thus also in σ_{xz} and u—see Sect. 2.5.8 which deals with power profiles. The loss of mechanical energy is, according to (4.42),

$$W_R(c,a) = -\frac{2[\mu E^* b\kappa(n)]^2}{G^*}\int_c^a (a^n - x^n)(x^n - c^n)\mathrm{d}x$$
$$= -\frac{2[\mu E^* b\kappa(n)]^2}{G^*}\frac{n}{n+1}\left[\frac{a^{2n+1} - c^{2n+1}}{2n+1} - a^n c^n(a-c)\right]. \quad (4.69)$$

This can be shown in normalized variables as

$$\eta := \frac{|W_R|}{\mu F_N u_c^{(0)}} = \frac{1}{2n+1}\left[1 - \left(\frac{c}{a}\right)^{2n+1}\right] - \left(\frac{c}{a}\right)^n\left(1 - \frac{c}{a}\right). \quad (4.70)$$

with the maximum

$$\eta_{\max} = \eta(c=0) = \frac{1}{2n+1}. \quad (4.71)$$

Since n must be a positive number, this only assumes values between zero and one, which of course is physically necessary. In Fig. 4.12 the expression $\eta/\eta_{\max}$ is represented as a function of c/a for different exponents n. It can be seen that the curves for larger exponents decrease with increasing radius of the stick zone later and are steeper against zero.

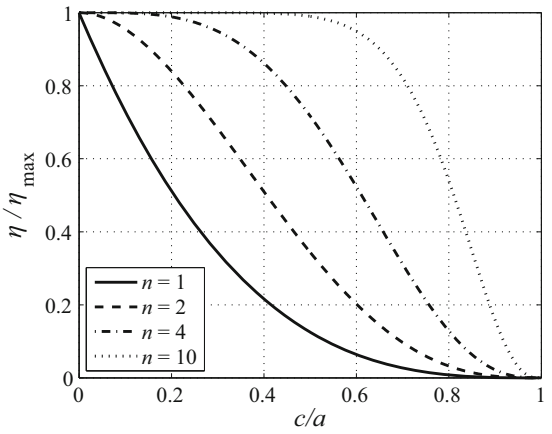

Fig. 4.12 Normalized dissipated friction energy as a function of the normalized radius of the stick zone during indentation by a power-law profile for different exponents n

4.6.5 The Truncated Cone

Now consider profiles that have a flat tip, for example, due to wear.

$$f(r) = \begin{cases} 0, & r \leq b, \\ (r-b)\tan\theta, & r > b. \end{cases} \tag{4.72}$$

Here, θ denotes the slope angle of the cone and b the radius at the blunt end. In Chap. 2 (Sect. 2.5.9) the following relationships between the global contact variables (indentation depth d, the contact radius a, and the normal force F_N) were derived for the solution of the normal contact problem:

$$\begin{aligned} d(a) &= a\tan\theta \arccos\left(\frac{b}{a}\right), \\ F_N(a) &= E^* \tan\theta a^2 \left[\arccos\left(\frac{b}{a}\right) + \frac{b}{a}\sqrt{1-\frac{b^2}{a^2}}\right]. \end{aligned} \tag{4.73}$$

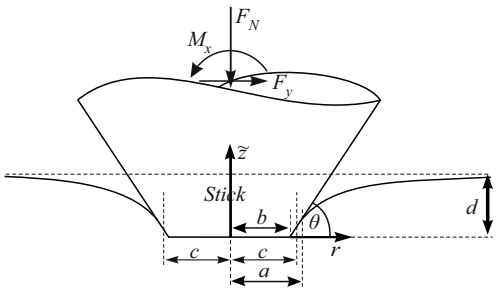

Fig. 4.13 Tangential contact between a rigid truncated cone and an elastic half-space

The mean pressure in contact is thus

$$p_0 = \frac{E^* \tan\theta}{\pi}\left[\arccos\left(\frac{b}{a}\right) + \frac{b}{a}\sqrt{1-\frac{b^2}{a^2}}\right]. \tag{4.74}$$

The equations for the normal stresses σ_{zz} and the displacements w of the half-space outside the contact region are described by the expressions:

$$\sigma_{zz}(r;a) = -\frac{E^* \tan\theta}{\pi}\begin{cases} \mathrm{K}\left(\frac{r}{b}\right) - \mathrm{F}\left(\arcsin\left(\frac{b}{a}\right), \frac{r}{b}\right) \\ \quad + \int_b^a \arccos\left(\frac{b}{x}\right)\frac{\mathrm{d}x}{\sqrt{x^2-r^2}}, & r \le b, \\ \frac{b}{r}\left[\mathrm{K}\left(\frac{b}{r}\right) - \mathrm{F}\left(\arcsin\left(\frac{r}{a}\right), \frac{b}{r}\right)\right] \\ \quad + \int_r^a \arccos\left(\frac{b}{x}\right)\frac{\mathrm{d}x}{\sqrt{x^2-r^2}}, & b < r \le a. \end{cases} \tag{4.75}$$

and

$$w(r;a) = \frac{2\tan\theta}{\pi}\left[\varphi_0 \mathrm{a}\arcsin\left(\frac{a}{r}\right) - \int_b^a x \arccos\left(\frac{b}{x}\right)\frac{\mathrm{d}x}{\sqrt{r^2-x^2}}\right], \quad r > a. \tag{4.76}$$

Here, $\mathrm{K}(\cdot)$ und $\mathrm{F}(\cdot,\cdot)$ denote the complete and incomplete elliptic integrals of the first kind:

$$\mathrm{K}(k) := \int_0^{\pi/2} \frac{\mathrm{d}\varphi}{\sqrt{1-k^2\sin^2\varphi}},$$
$$\mathrm{F}(\alpha,k) := \int_0^{\alpha} \frac{\mathrm{d}\varphi}{\sqrt{1-k^2\sin^2\varphi}}. \tag{4.77}$$

By applying (4.38), the tangential contact problem (see Fig. 4.13) can now be solved. For the tangential displacement $u^{(0)}$ and the tangential force F_x, one obtains:

$$u^{(0)}(a,c) = \frac{\mu E^*}{G^*}\tan\theta\left[a\arccos\left(\frac{b}{a}\right) - c\arccos\left(\frac{b}{c}\right)\right],$$
$$F_x(a,c) = \mu E^* \tan\theta\left\{a^2\left[\arccos\left(\frac{b}{a}\right) + \frac{b}{a}\sqrt{1-\frac{b^2}{a^2}}\right]\right.$$
$$\left. - c^2\left[\arccos\left(\frac{b}{c}\right) + \frac{b}{c}\sqrt{1-\frac{b^2}{c^2}}\right]\right\}. \tag{4.78}$$

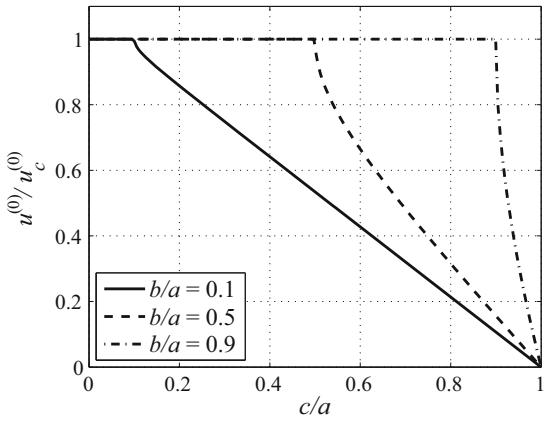

Fig. 4.14 Normalized tangential displacement as a function of the normalized radius of the stick zone for different values b/a during indentation by a truncated cone

The radius of the stick zone c cannot decrease below the value of b; the contact starts to slide completely, if $b = c$. The corresponding maximum tangential displacement is described by:

$$u_c^{(0)}(a) = \frac{\mu E^* a}{G^*} \tan\theta \arccos\left(\frac{b}{a}\right). \tag{4.79}$$

It is easy to see that $b = 0$ reproduces results of the complete cone. In Fig. 4.14 the normalized tangential displacement $u^{(0)}/u_c^{(0)}$ is shown as a function of the normalized radius of the stick zone c/a for different values of b/a. It can be seen that the curves for very small values of b approach the solution of the complete cone

$$\lim_{b\to 0} \frac{u^{(0)}}{u_c^{(0)}} = 1 - \frac{c}{a}. \tag{4.80}$$

Figure 4.15 shows the dependency on c/a for the normalized tangential force $F_R/(\mu F_N)$. Again, the limiting curve corresponding to the whole cone is easily recognizable:

$$\lim_{b\to 0} \frac{F_R}{\mu F_N} = 1 - \frac{c^2}{a^2}. \tag{4.81}$$

The tangential stresses and displacements can be obtained by substituting the results obtained so far in this section into (4.38). Figures 4.16 and 4.17 show the normalized curves of the tangential stress in contact for different values of the normalized radius of the stick zone at $b = 0.09a$ and $b = 0.49a$. For $b = 0.09a$, the result hardly differs from the curves of the complete cone in Fig. 4.4. It can be seen that $c > b$. Thus, before the complete sliding begins, the tangential stresses (in contrast to the pressure distribution) has no singularities. For $b = c$, i.e., at the beginning of complete sliding, is $|\sigma_{xz}| = \mu|\sigma_{zz}|$, which means that the tangential stresses at $r = b$ have the same singular behavior as the normal stresses.

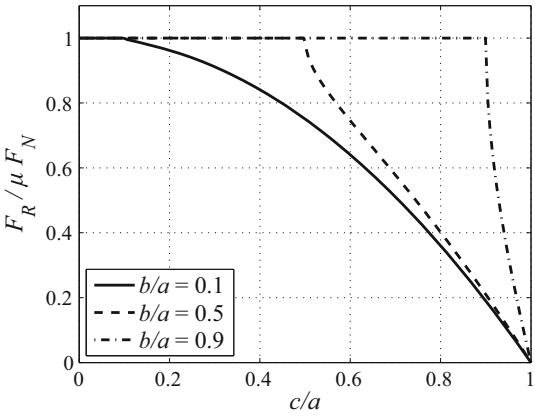

Fig. 4.15 Normalized tangential force as a function of the normalized radius of the stick zone for different values during indentation by a truncated cone

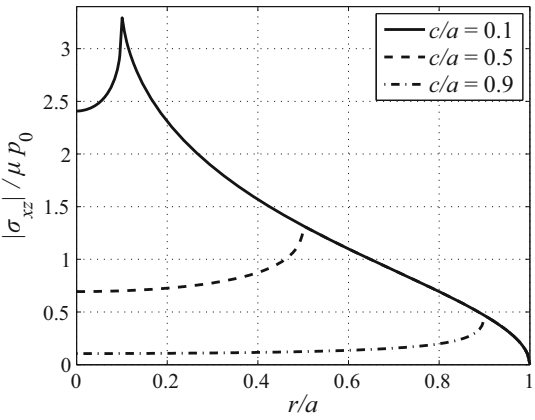

Fig. 4.16 Normalized tangential stresses in contact for different values of the normalized radius of the stick zone c/a during indentation by a truncated cone with $b = 0.09a$

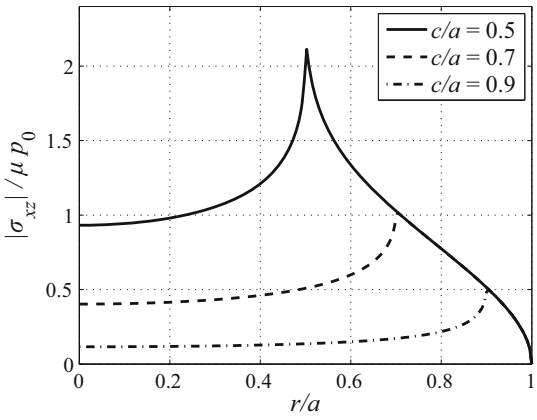

Fig. 4.17 Normalized tangential stresses in contact for different values of the normalized radius of the stick zone c/a during indentation by a truncated cone with $b = 0.49a$

4.6.6 The Truncated Paraboloid

A truncated paraboloid with the radius of curvature R and the radius at the flat tip b can be described by the profile

$$f(r) = \begin{cases} 0, & r \le b, \\ \frac{r^2 - b^2}{2R}, & r > b. \end{cases} \tag{4.82}$$

In Chap. 2 in Sect. 2.5.10, the solution

$$\begin{aligned} d(a) &= \frac{a}{R}\sqrt{a^2 - b^2}, \\ F_N(a) &= \frac{2E^*}{3R}(2a^2 + b^2)\sqrt{a^2 - b^2} \end{aligned} \tag{4.83}$$

for the normal contact problem was determined. Here, as always, d denotes the depth of indentation, a the contact radius, and F_N the normal force. The stresses were given in integral form as:

$$\sigma_{zz}(r;a) = -\frac{E^*}{\pi R} \begin{cases} \displaystyle\int_b^a \frac{(2x^2 - b^2)\mathrm{d}x}{\sqrt{x^2 - b^2}\sqrt{x^2 - r^2}}, & r \le b, \\ \displaystyle\int_r^a \frac{(2x^2 - b^2)\mathrm{d}x}{\sqrt{x^2 - b^2}\sqrt{x^2 - r^2}}, & b < r \le a. \end{cases} \tag{4.84}$$

and for the normal off-contact displacements:

$$\begin{aligned} w(r;a) = {} & \frac{2a}{\pi R}\sqrt{a^2 - b^2}\arcsin\left(\frac{a}{r}\right) \\ & - \frac{1}{\pi R}\left[(r^2 - b^2)\arcsin\left(\frac{\sqrt{a^2 - b^2}}{\sqrt{r^2 - b^2}}\right) - \sqrt{a^2 - b^2}\sqrt{r^2 - a^2}\right], \\ & r > a. \end{aligned} \tag{4.85}$$

was found.

Thus, for the tangential contact problem (see Fig. 4.18), the following relationships between the global contact variables (tangential displacement of the indenter $u^{(0)}$, radius of the stick zone c, and tangential force F_x) can be determined using (4.38) (the contact starts to slide completely at $b = c$):

$$\begin{aligned} u^{(0)}(a,c) &= \frac{\mu E^*}{G^* R}\left(a\sqrt{a^2 - b^2} - c\sqrt{c^2 - b^2}\right), \\ u_c^{(0)}(a) &= \frac{\mu E^*}{G^* R} a\sqrt{a^2 - b^2}, \\ F_x(a,c) &= \frac{2\mu E^*}{3R}\left[(2a^2 + b^2)\sqrt{a^2 - b^2} - (2c^2 + b^2)\sqrt{c^2 - b^2}\right]. \end{aligned} \tag{4.86}$$

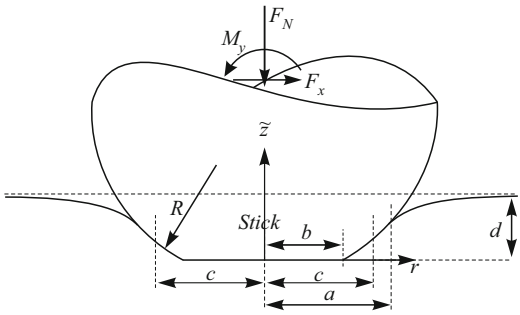

Fig. 4.18 Tangential contact between a rigid truncated paraboloid and an elastic half-space

These are shown in a normalized manner in Figs. 4.19 and 4.20. As in the case of the truncated cone, for small values of b, it is easy to reproduce the known limiting cases of the complete paraboloid; namely:

$$\lim_{b\to 0}\left[\frac{u^{(0)}}{u_c^{(0)}}\right] = 1 - \frac{c^2}{a^2} \tag{4.87}$$

and

$$\lim_{b\to 0}\left[\frac{F_x}{\mu F_N}\right] = 1 - \frac{c^3}{a^3}. \tag{4.88}$$

The tangential stresses and displacements should, again, not be written out for reasons of space but can be obtained by inserting them into the general equations (4.38). Some dependencies of the tangential stresses are shown in Figs. 4.21 and 4.22. These have the same singular behavior as in the case of the truncated cone; that is, the tangential stresses are only singular if $r = b = c$, i.e., in case of full sliding.

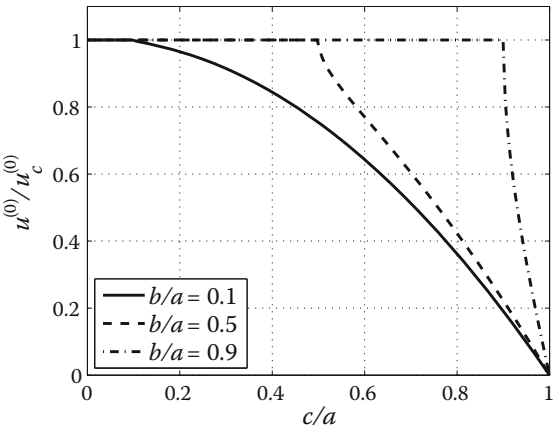

Fig. 4.19 Normalized tangential displacement as a function of the normalized radius of the stick zone for different values b/a when indented by a truncated paraboloid

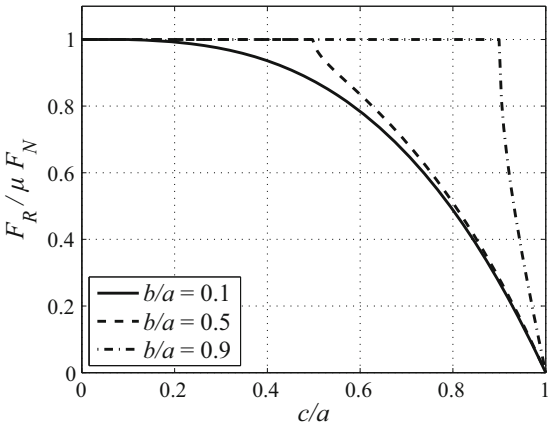

Fig. 4.20 Normalized tangential displacement as a function of the normalized radius of the stick zone for different values b/a when indented by a truncated paraboloid

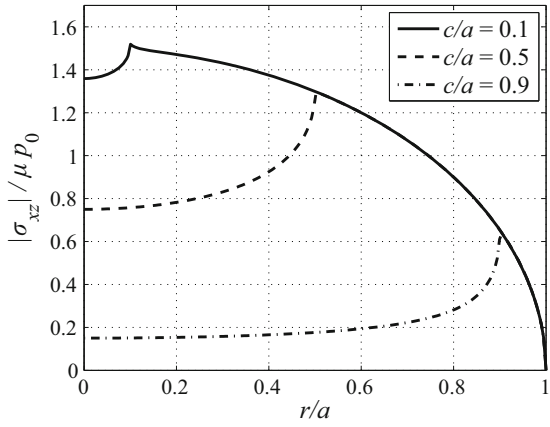

Fig. 4.21 Normalized tangential stresses in the contact for different values of the normalized radius of the stick zone c/a when indented by a truncated paraboloid with $b = 0.09a$

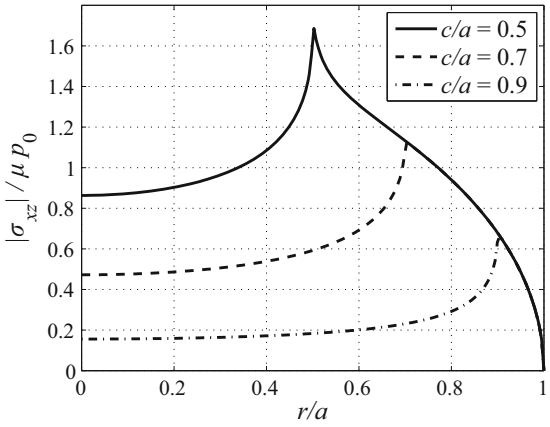

Fig. 4.22 Normalized tangential stresses in the contact for different values of the normalized radius of the stick zone c/a when indented by a truncated paraboloid with $b = 0.49a$

4.6.7 The Cylindrical Flat Punch with Parabolic Cap

For the consideration of the indenter with parabolic cap (see Fig. 4.23) we assume, as always, that the indentation depth d is large enough to actually bring the main body into contact. Otherwise it would be the pure contact with a paraboloid, for which the results can be looked up in Sect. 4.6.3. The flat cylindrical punch with a parabolic cap can be described by the profile:

$$f(r) = \begin{cases} \dfrac{r^2}{2R}, & r \le a, \\ \infty, & r > a. \end{cases} \tag{4.89}$$

Here, a is the radius of the punch and R is the radius of curvature of the cap. In cases where d is indeed sufficiently large, the solution of the friction-free normal contact problem (with the normal force F_N, the stress distribution σ_{zz} within, and the normal displacements of the half-space w outside the contact) was derived in Chap. 2 in Sect. 2.5.11, to which we want to refer again.

$$\begin{aligned} F_N(d) &= 2E^* \left(da - \frac{a^3}{3R} \right), \quad dR \ge a^2, \\ \sigma_{zz}(r;d) &= -\frac{E^*}{\pi R} \frac{a^2 - 2r^2 + dR}{\sqrt{a^2 - r^2}}, \quad r \le a,\ dR \ge a^2, \\ w(r;d) &= \frac{1}{\pi R} \left[(2dR - r^2) \arcsin\left(\frac{a}{r}\right) + a\sqrt{r^2 - a^2} \right], \\ & \qquad r > a,\ dR \ge a^2. \end{aligned} \tag{4.90}$$

The mean pressure in contact is:

$$p_0 = \frac{F_N}{\pi a^2} = \frac{2E^*}{3\pi R a}(3dR - a^2). \tag{4.91}$$

Since the normal stress at the edge of the contact at $r = a$ is singular, the contact can stick completely even after applying a tangential force, as in the case of the flat

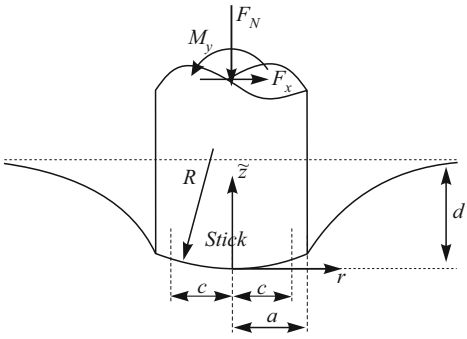

Fig. 4.23 Tangential contact between a rigid cylindrical punch with parabolic cap and an elastic half-space

punch. The exact MDR shape of the problem makes it easy to understand how long this condition can last. The springs on the edge of the contact will begin to slide, if

$$u^{(0)} > \frac{\mu E^*}{G^*}\left(d - \frac{a^2}{R}\right) := u_1^{(0)}. \tag{4.92}$$

Thereafter, the area of partial sliding begins to spread from the edge until finally the whole contact slides, if

$$u^{(0)} > \frac{\mu E^*}{G^*} d := u_c^{(0)}. \tag{4.93}$$

In contrast to all previous sections of this chapter, there are three different regimes:

- $u^{(0)} \le u_1^{(0)}$: complete sticking
- $u_1^{(0)} < u^{(0)} < u_c^{(0)}$: partial sliding
- $u^{(0)} \ge u_c^{(0)}$: complete sliding

The corresponding solutions of the tangential contact problem, i.e., the relationships between the radius of the stick zone c, the tangential displacement of the indenter $u^{(0)}$, the tangential force F_x, and the tangential stresses σ_{xz} and displacements u of the half-space are given by the general relations (3.38) as follows.

Case 1: Complete Sticking

$$\begin{aligned} F_x(u^{(0)}) &= 2G^* a u^{(0)}, \\ \sigma_{xz}(r; u^{(0)}) &= -\frac{G^* u^{(0)}}{\pi\sqrt{a^2 - r^2}}, \quad r \le a \\ u(r; u^{(0)}) &= \frac{2u^{(0)}}{\pi}\arcsin\left(\frac{a}{r}\right), \quad r > a. \end{aligned} \tag{4.94}$$

Case 2: Partial Sliding with Radius of the Stick Zone c

$$\begin{aligned} u^{(0)}(d,c) &= \frac{\mu E^*}{G^*}\left(d - \frac{c^2}{R}\right), \\ F_x(d,c) &= \frac{2\mu E^*}{3R}\left(3adR - a^3 - 2c^3\right), \\ \sigma_{xz}(r;d,c) &= -\frac{\mu E^*}{\pi R}\begin{cases} 2\sqrt{a^2 - r^2} - 2\sqrt{c^2 - r^2} + \dfrac{dR - a^2}{\sqrt{a^2 - r^2}}, & r \le c, \\ 2\sqrt{a^2 - r^2} + \dfrac{dR - a^2}{\sqrt{a^2 - r^2}}, & c < r \le a, \end{cases} \end{aligned}$$

$$u(r;d,c)=\frac{\mu E^*}{G^*R}\begin{cases} dR-\dfrac{r^2}{2}-\dfrac{1}{\pi}\Big[\left(2c^2-r^2\right)\arcsin\left(\dfrac{c}{r}\right) & \\ \qquad\qquad +c\sqrt{r^2-c^2}\Big], & c<r\le a,\\ \dfrac{1}{\pi}\Big[\left(2dR-r^2\right)\arcsin\left(\dfrac{a}{r}\right) & \\ \quad +a\sqrt{r^2-a^2}-\left(2c^2-r^2\right)\arcsin\left(\dfrac{c}{r}\right) & \\ \quad -c\sqrt{r^2-c^2}\Big], & r>a. \end{cases} \tag{4.95}$$

The normalized tangential stresses and displacements are shown for the case $dR = 1.2a^2$ in Figs. 4.24 and 4.25. When using the Ciavarella–Jäger principle in the form

$$\sigma_{xz}(r)=\mu\left[\sigma_{zz}(r;a)-\sigma_{zz}(r;c)\right], \tag{4.96}$$

care should be taken. $\sigma_{zz}(r;c)$ denotes the stress distribution which arises when the *same* indenter (i.e., with the punch radius a), is pressed into the half-space up to a contact radius c. But this means only the parabolic cap is in contact, so the stress distribution is the stress distribution of the simple paraboloid going back to Hertz (1882):

$$\sigma_{zz}(r;c)=-\frac{2E^*}{\pi R}\sqrt{c^2-r^2}\neq\sigma_{zz}(r;a)|_{a=c}\,. \tag{4.97}$$

This blurring of the notation is hard to avoid. The same applies to $w\,(r;c)$, which is required for the calculation of the tangential displacement distribution according to (4.38).

Case 3: Complete Sliding

In the case of complete sliding, the solution results by substituting $c = 0$ into (4.95). For $R \to \infty$, the case of the flat cylindrical punch results. Then the possibility of partially sliding is eliminated because of $u_1^{(0)} = u_c^{(0)}$.

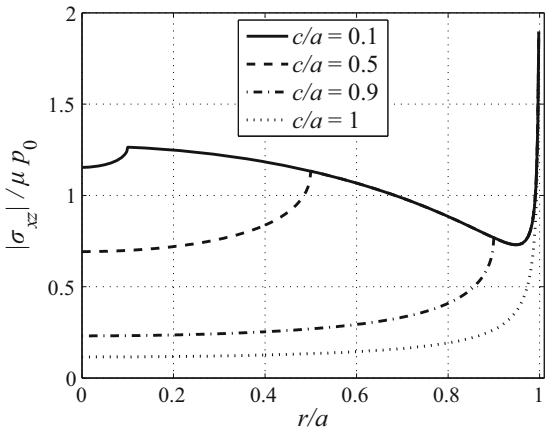

Fig. 4.24 Normalized tangential stresses during indentation by a flat stamp with paraboloidal cap for $dR = 1.2a^2$ and different values of the normalized radius of the stick zone. The dotted line corresponds to the case $u^{(0)} = u_1^{(0)}$

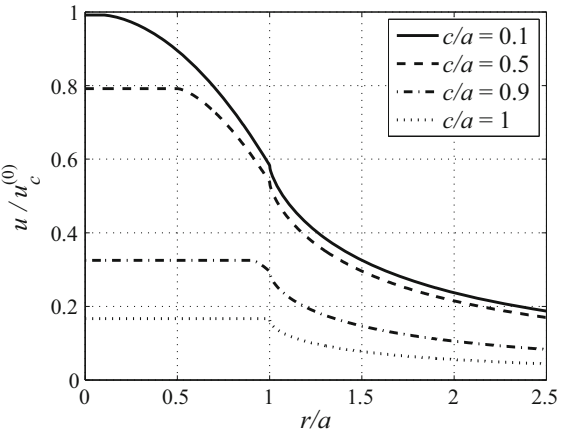

Fig. 4.25 Normalized tangential displacements when indented by a flat punch with paraboloidal cap for $dR = 1.2a^2$ and different values of the normalized radius of the stick zone. The dotted line corresponds to the case $u^{(0)} = u_1^{(0)}$

4.6.8 The Cone with Parabolic Cap

The tangential contact between a cone with a rounded tip and an elastic half-space, shown schematically in Fig. 4.26, was first investigated and solved by Ciavarella (1999). The profile of the indenter with the conical slope angle θ and the value of b of the radial coordinate at which the conical main body differentiably passes into the parabolic cap is described by the rule

$$f(r) = \begin{cases} \dfrac{r^2 \tan\theta}{2b}, & r \le b, \\ r\tan\theta - \dfrac{b}{2}\tan\theta, & r > b. \end{cases} \tag{4.98}$$

In Chap. 2 (see Sect. 2.5.12) the following solution for the normal contact problem was derived:

$$\begin{aligned} d(a) &= a\tan\theta\left(\frac{1-\sin\varphi_0}{\cos\varphi_0} + \varphi_0\right), \\ F_N(a) &= E^* a^2 \tan\theta\left(\varphi_0 + \frac{4}{3}\frac{1-\sin\varphi_0}{\cos\varphi_0} + \frac{1}{3}\sin\varphi_0\cos\varphi_0\right), \end{aligned} \tag{4.99}$$

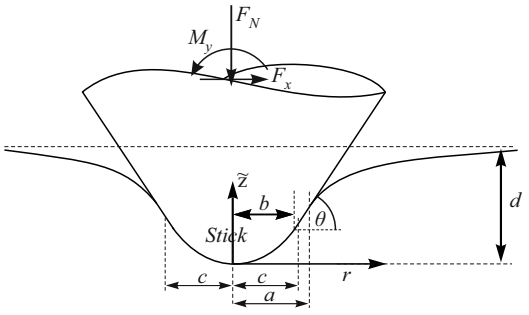

Fig. 4.26 Tangential contact between a rigid cone with a rounded tip and an elastic half-space

with

$$\varphi_0 := \arccos\left(\frac{b}{a}\right), \tag{4.100}$$

The contact is radius a, the indentation depth d, and normal force F_N. The normal stresses in the contact are described by:

$$\sigma_{zz}(r;a) = -\frac{E^* \tan\theta}{\pi b} \begin{cases} 2\sqrt{a^2 - r^2} \\ \quad + b \int_0^{\varphi_0} \dfrac{(\varphi - 2\tan\varphi)\tan\varphi \, \mathrm{d}\varphi}{\sqrt{1 - k^2 \cos^2\varphi}}, & r \le b, \\ 2\sqrt{a^2 - r^2} \\ \quad + b \int_0^{\operatorname{arcosh}\left(\frac{a}{r}\right)} \left[\arccos\left(\dfrac{b}{r\cosh\varphi}\right) \right. \\ \qquad \left. - 2\sqrt{k^2 \cosh^2\varphi - 1} \right] \mathrm{d}\varphi, & b < r \le a \end{cases} \tag{4.101}$$

and the normal displacements out of contact through the distribution:

$$\begin{aligned} w(r;a) = & \\ & \frac{2d(a)}{\pi} \arcsin\left(\frac{a}{r}\right) \\ & - \frac{\tan\theta}{\pi b} \left[r^2 \arcsin\left(\frac{a}{r}\right) - a\sqrt{r^2 - a^2} + 2b^2 \int_0^{\varphi_0} \frac{(\varphi - \tan\varphi)\tan\varphi \mathrm{d}\varphi}{\cos\varphi \sqrt{k^2 \cos^2\varphi - 1}} \right], \\ & r > a. \end{aligned} \tag{4.102}$$

It is assumed that the contact radius does not fall below the value $a = b$. If $a < b$, it is the contact with a paraboloid with the radius of curvature,

$$R := \frac{b}{\tan\theta}, \tag{4.103}$$

for which the results can be looked up in Sect. 4.6.3. If the normal stress at the edge of the contact disappears, the contact cannot fully stick at a tangential load. There are three different cases for the sliding regime:

- partial sliding with $c > b$
- partial sliding with $c \le b$
- complete sliding

Equations (4.38) can be used to obtain the following solutions to the tangential contact problem (radius of the stick zone c, tangential indenter displacement $u^{(0)}$, tangential force F_R, tangential stresses σ_{xz}, and half-space displacements u):

Case 1: Partial Sliding with $c > b$

$$u^{(0)}(a,c) = \frac{\mu E^*}{G^*}\tan\theta\left[a\left(\frac{1-\sin\varphi_0}{\cos\varphi_0}+\varphi_0\right)-c\left(\frac{1-\sin\psi_0}{\cos\psi_0}+\psi_0\right)\right],$$

$$F_x(a,c) = \mu E^*\tan\theta\left[a^2\left(\varphi_0+\frac{4}{3}\frac{1-\sin\varphi_0}{\cos\varphi_0}+\frac{1}{3}\sin\varphi_0\cos\varphi_0\right)\right.$$
$$\left.-c^2\left(\psi_0+\frac{4}{3}\frac{1-\sin\psi_0}{\cos\psi_0}+\frac{1}{3}\sin\psi_0\cos\psi_0\right)\right],$$

$$\sigma_{xz}(r;a,c) = \mu\begin{cases}\sigma_{zz}(r;a)-\sigma_{zz}(r;c), & r\le c,\\ \sigma_{zz}(r;a), & c<r\le a,\end{cases}$$

$$u(r;a,c) = \frac{\mu E^*}{G^*}\begin{cases}d(a)-f(r)-w(r;c), & c<r\le a,\\ w(r;a)-w(r;c), & r>a,\end{cases} \tag{4.104}$$

with

$$\psi_0 := \arccos\left(\frac{b}{c}\right). \tag{4.105}$$

In this case (in contrast to the previous section), $\sigma_{zz}(r;c)$ actually means $\sigma_{zz}(r;a)|_{a=c}$. This also applies analogously for all other expressions. Therefore, all functions that are still open in (4.104) can be looked up in (4.98) to (4.102). For $b = 0$ and, therefore, $\varphi_0 = \psi_0 = \pi/2$; the solutions for the complete cone from Sect. 4.6.2 are recovered.

Case 2: Partial Sliding with $c \le b$

The principle of Ciavarella and Jäger demands at this point that the solution of the tangential contact problem is given by the difference of solutions of the following two normal contact problems: firstly, the normal indentation by the indenter defined in (4.98) up to a contact radius a, and secondly, the normal indentation of the same indenter up to a contact radius $c \le b$. The latter corresponds to a normal contact with a paraboloid, since only the parabolic tip of the indenter is in contact. So the tangential solution we are looking for is:

$$u^{(0)}(a,c) = \frac{\mu E^*}{G^*}\tan\theta\left[a\left(\frac{1-\sin\varphi_0}{\cos\varphi_0}+\varphi_0\right)-\frac{c^2}{b}\right],$$

$$F_x(a,c) = \mu E^*\tan\theta\left[a^2\left(\varphi_0+\frac{4}{3}\frac{1-\sin\varphi_0}{\cos\varphi_0}+\frac{1}{3}\sin\varphi_0\cos\varphi_0\right)-\frac{4c^3}{3b}\right],$$

$$\sigma_{xz}(r;a,c) = \mu\begin{cases}\sigma_{zz}(r;a)+\dfrac{2E^*}{\pi b}\tan\theta\sqrt{c^2-r^2}, & r\le c,\\ \sigma_{zz}(r;a), & c<r\le a,\end{cases}$$

$$u(r;a,c) = \frac{\mu E^*}{G^*}\begin{cases}d(a)-f(r)-w_p(r;c), & c<r\le a,\\ w(r;a)-w_p(r;c), & r>a,\end{cases} \tag{4.106}$$

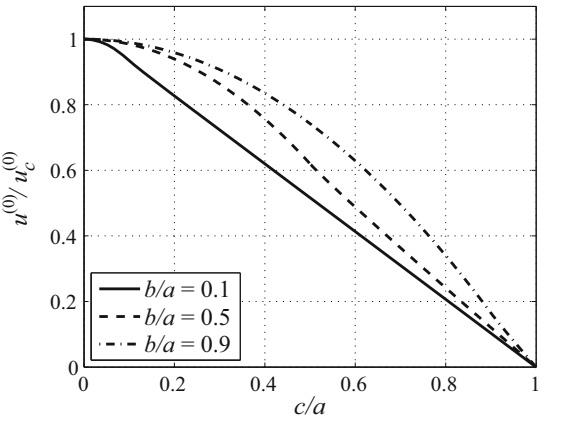

Fig. 4.27 Normalized tangential displacement as a function of the normalized radius of the stick zone for different values b/a when indenting by a cone with a rounded tip

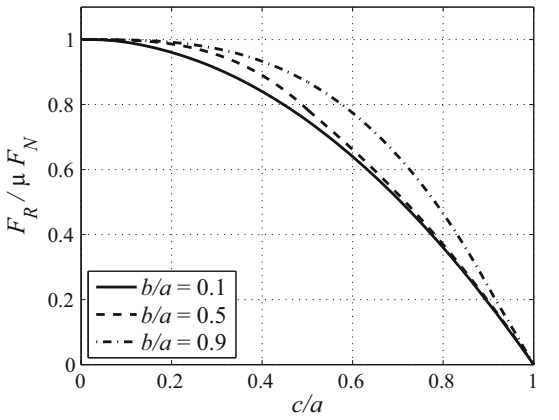

Fig. 4.28 Normalized tangential displacement as a function of the normalized radius of the stick zone for different values b/a when indenting by a cone with a rounded tip

with the displacement:

$$w_p(r;c) = \frac{c^2}{\pi b}\tan\theta\left[\left(2-\frac{r^2}{c^2}\right)\arcsin\left(\frac{c}{r}\right)+\frac{\sqrt{r^2-c^2}}{c}\right]. \tag{4.107}$$

Case 3: Complete Sliding

The solution here is a result of inserting $c = 0$ into solutions (4.106).

Figure 4.27 and 4.28 show the normalized values of the global contact sizes $u^{(0)}$ and F_R as a function of the normalized radius of the stick zone. For small values of b, one recognizes very well the limiting case of the ideal cone.

The curves of the normalized tangential stresses for individual normalized values of the two radii b and c are shown in Figs. 4.29 and 4.30. It is immediately apparent that for small values of b the curves of the ideal cone can be found. However, one also sees that the dependency for $c > b$ only weakly depends on b. For example, the curve of $c = 0.9a$ and $b = 0.5a$ is almost exactly that of the ideal cone at $c = 0.9a$, despite the rather large value of b.

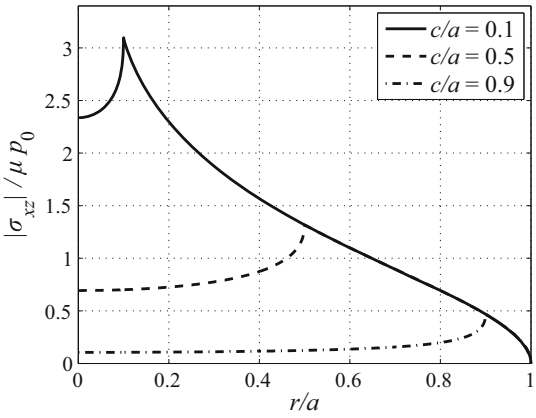

Fig. 4.29 Normalized tangential stresses in the indentation by a cone with a rounded tip for $b = 0.1a$ and different values of the normalized radius of the stick zone

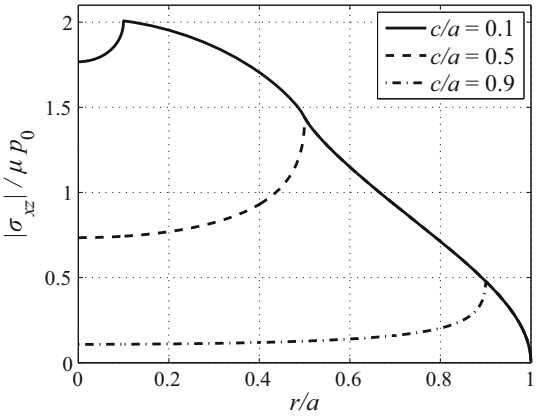

Fig. 4.30 Normalized tangential stresses in the indentation by a cone with a rounded tip for $b = 0.5a$ and different values of the normalized radius of the stick zone

4.6.9 The Paraboloid with Parabolic Cap

The method in this problem is completely analogous to that of the previous sections. The indenter profile can be described by the function:

$$f(r) = \begin{cases} \dfrac{r^2}{2R_1}, & r \le b, \\ \dfrac{r^2 - h^2}{2R_2}, & r > b. \end{cases} \tag{4.108}$$

Here, R_1 is the radius of curvature of the parabolic cap, and R_2 is the radius of the parabolic base body (see Fig. 4.31). The continuity of f implies

$$h^2 = b^2 \left(1 - \frac{R_2}{R_1}\right) \tag{4.109}$$

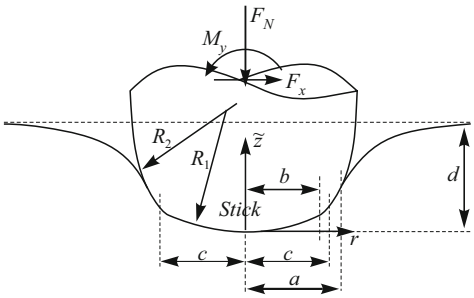

Fig. 4.31 Tangential contact between a rigid paraboloid with parabolic cap and an elastic half-space

for the length h. The normal contact problem with a contact radius $a \geq b$, the indentation depth d, the normal force F_N, and the normal stresses and displacements of the half-space σ_{zz} and w is described by the relations:

$$
\begin{aligned}
d(a) &= \frac{a^2}{R_1} + \frac{a}{R^*}\sqrt{a^2-b^2}, \\
F_N(a) &= \frac{2E^*}{3}\left[\frac{2a^3}{R_1} + \frac{1}{R^*}\left(2a^2+b^2\right)\sqrt{a^2-b^2}\right], \\
\sigma_{zz}(r;a) &= -\frac{E^*}{\pi}\begin{cases} \dfrac{2\sqrt{a^2-r^2}}{R_1} + \displaystyle\int_b^a \frac{\left(2x^2-b^2\right)\mathrm{d}x}{R^*\sqrt{x^2-b^2}\sqrt{x^2-r^2}}, & r \leq b, \\ \dfrac{2\sqrt{a^2-r^2}}{R_1} + \displaystyle\int_r^a \frac{\left(2x^2-b^2\right)\mathrm{d}x}{R^*\sqrt{x^2-b^2}\sqrt{x^2-r^2}}, & b < r \leq a, \end{cases} \\
w(r;a) &= w_P(r;a;R=R_1) + w_{PS}(r;a;R=R^*), \quad r > a,
\end{aligned}
\tag{4.110}
$$

derived in Sect. 2.5.13. Here, w_P and w_{PS} denote the displacements in the indentation by a complete or truncated paraboloid:

$$
\begin{aligned}
w_P(r;a;R_1) &= \frac{a^2}{\pi R_1}\left[\left(2-\frac{r^2}{a^2}\right)\arcsin\left(\frac{a}{r}\right) + \frac{\sqrt{r^2-a^2}}{a}\right], \\
w_{PS}(r;a;R^*) &= \frac{2a}{\pi R^*}\sqrt{a^2-b^2}\arcsin\left(\frac{a}{r}\right) \\
&\quad - \frac{1}{\pi R^*}\left[\left(r^2-b^2\right)\arcsin\left(\frac{\sqrt{a^2-b^2}}{\sqrt{r^2-b^2}}\right) - \sqrt{a^2-b^2}\sqrt{r^2-a^2}\right].
\end{aligned}
\tag{4.111}
$$

R^* is an effective radius, which is described by the relation:

$$
R^* = \frac{R_1 R_2}{R_1 - R_2}. \tag{4.112}
$$

For $a < b$, we have a contact with a pure paraboloid with the radius of curvature R_1, for which the results can be looked up in Sect. 4.6.3. The solution of the tangential

contact problem in the three cases already introduced in the previous section is as follows (all open functions in (4.113) and (4.114) can be taken from (4.108) to (4.112). $u^{(0)}$ denotes the tangential displacement of the rigid indenter, c the radius of the stick zone, F_R the tangential force, σ_{xz} the tangential stresses, and u the tangential displacements on the surface of the half-space).

Case 1: Partial Sliding with $c > b$

$$
\begin{aligned}
u^{(0)}(a,c) &= \frac{\mu E^*}{G^*}\left(\frac{a^2}{R_1}+\frac{a}{R^*}\sqrt{a^2-b^2}-\frac{c^2}{R_1}-\frac{c}{R^*}\sqrt{c^2-b^2}\right),\\
F_x(a,c) &= \frac{2\mu E^*}{3}\left[\frac{2a^3}{R_1}+\frac{1}{R^*}(2a^2+b^2)\sqrt{a^2-b^2}\right.\\
&\qquad\left.-\frac{2c^3}{R_1}-\frac{1}{R^*}(2c^2+b^2)\sqrt{c^2-b^2}\right],\\
\sigma_{xz}(r;a,c) &= \mu\begin{cases}\sigma_{zz}(r;a)-\sigma_{zz}(r;c), & r\le c,\\ \sigma_{zz}(r;a), & c<r\le a,\end{cases}\\
u(r,a,c) &= \frac{\mu E^*}{G^*}\begin{cases}d(a)-f(r)-w(r;c), & c<r\le a,\\ w(r;a)-w(r;c), & r>a.\end{cases}
\end{aligned}
\tag{4.113}
$$

Case 2: Partial Sliding with $c \le b$

$$
\begin{aligned}
u^{(0)}(a,c) &= \frac{\mu E^*}{G^*}\left(\frac{a^2}{R_1}+\frac{a}{R^*}\sqrt{a^2-b^2}-\frac{c^2}{R_1}\right),\\
F_x(a,c) &= \frac{2\mu E^*}{3}\left[\frac{2a^3}{R_1}+\frac{1}{R^*}\left(2a^2+b^2\right)\sqrt{a^2-b^2}-\frac{2c^3}{R_1}\right],\\
\sigma_{xz}(r;a,c) &= \mu\begin{cases}\sigma_{zz}(r;a)+\dfrac{2E^*}{\pi R_1}\sqrt{c^2-r^2}, & r\le c,\\ \sigma_{zz}(r;a), & c<r\le a,\end{cases}\\
u(r;a,c) &= \frac{\mu E^*}{G^*}\begin{cases}d(a)-f(r)-w_p(r;c;R_1), & c<r\le a,\\ w(r;a)-w_p(r;c;R_1), & r>a.\end{cases}
\end{aligned}
\tag{4.114}
$$

Case 3: Complete Sliding

The solution arises here by inserting $c = 0$ into (4.114).

One obtains the usual limiting cases for this indenter profile: for $R_1 = R_2$, respectively $R^* \to \infty$, the solution of Cattaneo and Mindlin from Sect. 4.6.3 can be used, for $R_1 \to \infty$ the solution of the truncated paraboloid from Sect. 4.6.6 and for $b = 0$ the solution of Cattaneo and Mindlin with radius R_2.

Now let us visualize some of the results obtained from this. For the sake of simplicity, let us choose $R_1 = R^*$. However, all of the effects characteristic of the indenter profile described in this section occur with this limitation.

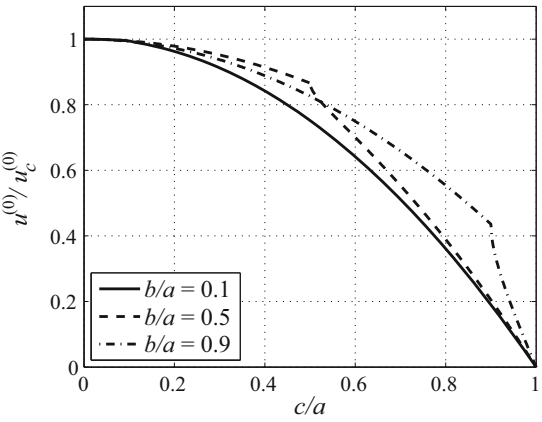

Fig. 4.32 Normalized tangential displacement as a function of the normalized radius of the stick zone for different values b/a when indented by a paraboloid with parabolic cap with $R_1 = R^*$

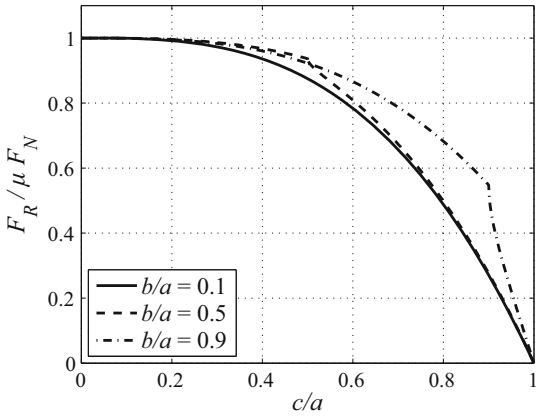

Fig. 4.33 Normalized tangential force as a function of the normalized stick radius for different values b/a when indented by a paraboloid with parabolic cap with $R_1 = R^*$

In Figs. 4.32 and 4.33 the normalized global tangential displacement $u^{(0)}$ and the normalized tangential force F_x are shown as a function of the normalized radius of the stick zone for different values of b. As always, one recognizes the characteristic limiting cases. In addition, one observes a kink at $c = b$, which has not yet appeared in the previous sections. This kink is due to the fact that the profile at $r = b$ is not continuously differentiable and yet radii of the stick zone $c < b$ are possible. This combination has not yet occurred in this chapter, or the kink corresponding to the transition to complete sliding of the contact.

Some normalized curves of the tangential stresses are shown in Figs. 4.34 and 4.35. As in the case of the cone with a rounded tip, the curves for $c > b$ barely differ from the dependencies for the ideal body; in this case the paraboloid from Sect. 4.6.3. In particular, the tangential stresses for $c > b$—in contrast to the normal stresses—are not singular at $r = b$.

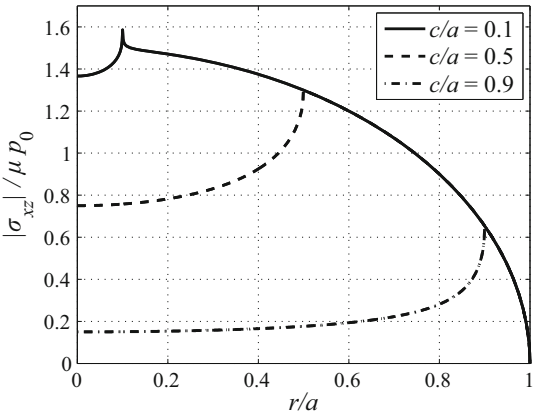

Fig. 4.34 Normalized tangential stresses when indented by a paraboloid with paraboloidal cap for $R_1 = R^*, b = 0.1a$ and different values of the normalized radius of the stick zone

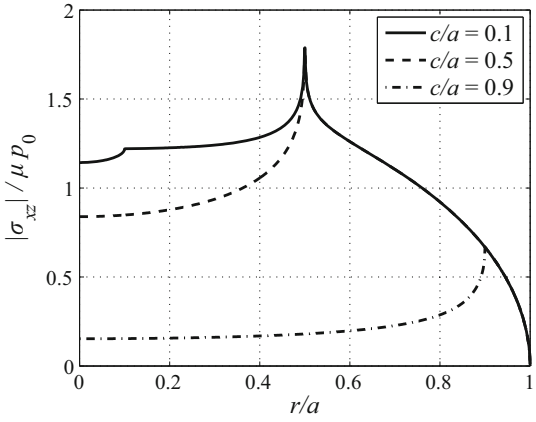

Fig. 4.35 Normalized tangential stresses when indented by a paraboloid with paraboloidal cap for $R_1 = R^*, b = 0.5a$ and different values of the normalized radius of the stick zone

4.6.10 The Cylindrical Flat Punch with a Rounded Edge

The tangential contact problem of a flat cylindrical punch with rounded corners and an elastic half-space (see Fig. 4.36) was first solved by Ciavarella (1999). The indenter profile has the shape

$$f(r) = \begin{cases} 0, & r \le b, \\ \dfrac{(r-b)^2}{2R}, & r > b, \end{cases} \tag{4.115}$$

with the radius of curvature R of the rounded corner and the radius b of the flat punch surface. The solution of the normal contact problem can be found in Chap. 2 (Sect. 2.5.14). As usual, a denotes the contact radius, d the indentation depth, and

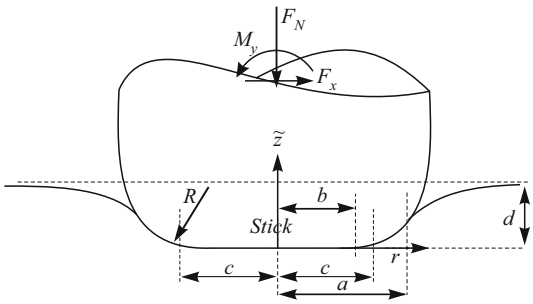

Fig. 4.36 Tangential contact between a rigid flat cylindrical punch with rounded corners and an elastic half-space

F_N the normal force. It is:

$$d(a) = \frac{a^2}{R}(\sin\varphi_0 - \varphi_0\cos\varphi_0),$$
$$F_N(a) = \frac{E^* a^3}{3R}\left[\sin\varphi_0(4-\cos^2\varphi_0) - 3\varphi_0\cos\varphi_0\right], \tag{4.116}$$

with the angle:

$$\varphi_0 := \arccos\left(\frac{b}{a}\right). \tag{4.117}$$

The stresses and displacements in the normal direction are:

$$\sigma_{zz}(r;a) = -\frac{E^*}{\pi R}\begin{cases}\displaystyle\int_b^a \left[2\sqrt{x^2-b^2} - b\arccos\left(\frac{b}{x}\right)\right]\frac{\mathrm{d}x}{\sqrt{x^2-r^2}}, & r \le b,\\ \displaystyle\int_r^a \left(2\sqrt{x^2-b^2} - b\arccos\left(\frac{b}{x}\right)\right)\frac{\mathrm{d}x}{\sqrt{x^2-r^2}}, & b < r \le a,\end{cases}$$
$$w(r;a) = \frac{2d(a)}{\pi}\arcsin\left(\frac{a}{r}\right) - \frac{2}{\pi}\left\{\int_b^a \frac{x}{R}\left[\sqrt{x^2-b^2} - b\arccos\left(\frac{b}{x}\right)\right]\frac{\mathrm{d}x}{\sqrt{r^2-x^2}}\right\},$$
$$r > a. \tag{4.118}$$

With a tangential loading of the contact, the radius of the stick zone cannot fall below the value of $c = b$, since the contact will begin to slide completely at this value. However, this makes it very easy to specify the solution of the tangential contact problem ($u^{(0)}$ denotes the tangential displacement of the rigid indenter, c the radius of the stick zone, F_x the tangential force, σ_{xz} the tangential stresses, and u the tangential displacements at the surface of the half-space). With help from the

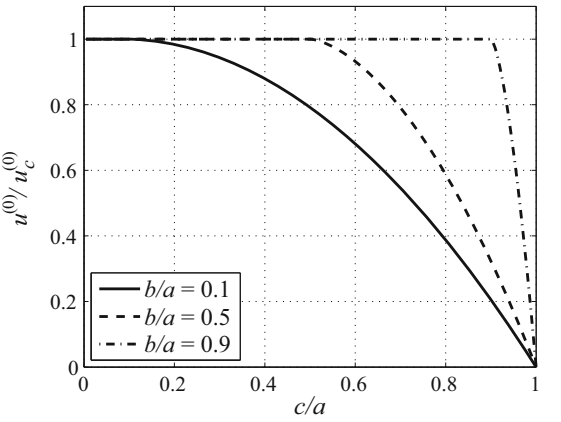

Fig. 4.37 Normalized tangential displacement as a function of the normalized radius of the stick zone for different values b/a when indenting with a flat punch with a rounded edge

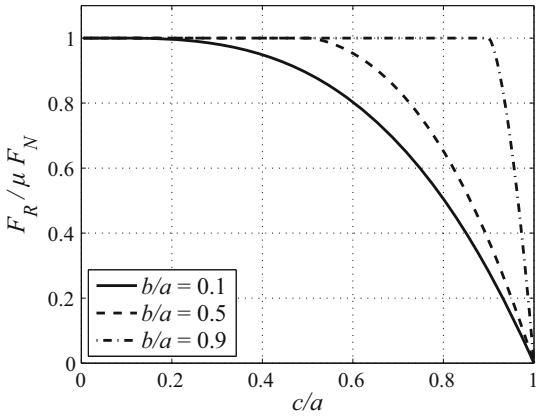

Fig. 4.38 Normalized tangential force as a function of the normalized radius of the stick zone for different values b/a when indenting with a flat punch with a rounded edge

general relations (4.38), one obtains:

$$
\begin{aligned}
u^{(0)}(a,c) &= \frac{\mu E^*}{G^* R}\left[a^2(\sin\varphi_0 - \varphi_0\cos\varphi_0) - c^2(\sin\psi_0 - \psi_0\cos\psi_0)\right],\\
F_x(a,c) &= \frac{E^*}{3R}\left\{a^3\left[\sin\varphi_0(4-\cos^2\varphi_0) - 3\varphi_0\cos\varphi_0\right]\right.\\
&\qquad \left. - c^3\left[\sin\psi_0(4-\cos^2\psi_0) - 3\psi_0\cos\psi_0\right]\right\},\\
\sigma_{xz}(r;a,c) &= \mu\begin{cases}\sigma_{zz}(r;a) - \sigma_{zz}(r;c), & r \le c,\\ \sigma_{zz}(r;a), & c < r \le a,\end{cases}\\
u(r;a,c) &= \frac{\mu E^*}{G^*}\begin{cases}d(a) - f(r) - w(r;c), & c < r \le a,\\ w(r;a) - w(r;c), & r > a,\end{cases}
\end{aligned}
\tag{4.119}
$$

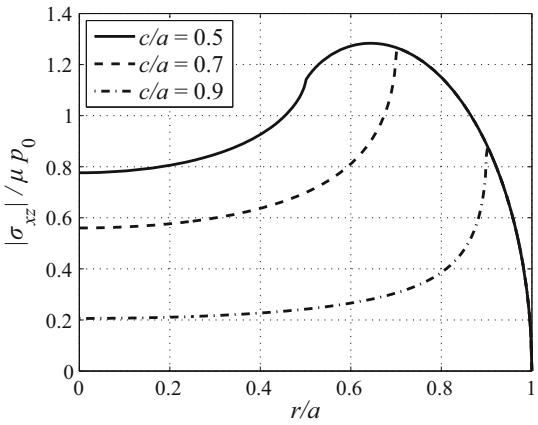

Fig. 4.39 Normalized tangential stresses in contact for different values of the normalized radius of the stick zone c/a, while indenting with a flat punch with rounded corners with $b = 0.49a$

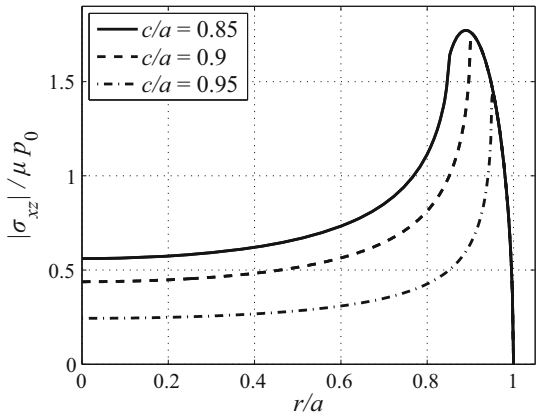

Fig. 4.40 Normalized tangential stresses in contact for different values of the normalized radius of the stick zone c/a, while indenting with a flat punch with rounded corners with $b = 0.84a$

with

$$\psi_0 := \arccos\left(\frac{b}{c}\right). \tag{4.120}$$

The solution for complete sliding is achieved by inserting $c = b$ into (4.119).

In Figs. 4.37 and 4.38 the tangential displacement and force are shown in normalized variables as functions of the normalized radius of the stick zone. Some curves of the tangential stresses are shown as an example in Figs. 4.39 and 4.40.

4.7 Adhesive Tangential Contact

In JKR theory, the equilibrium configuration of an adhesive contact is determined by minimizing the total energy of the system, which consists of the energy of the elastic deformation of the contact partners, the surface energy, and the work from external forces. Since this total energy does not depend on the tangential displacement, the JKR contact does not formally possess any "tangential strength". Strictly speaking, the absence of friction is one of the assumptions of the JKR solution, since it uses the solutions of the frictionless normal contact problem as its building blocks. Yet the lack of tangential strength of adhesive contacts is obviously contradicted by experimental results. The physical cause of this contradiction lies in the heterogeneous structure found at the microscopic scale (or at the atomic scale, at the very least) of any real interface. This heterogeneity leads to a finite contact strength (or static friction) in the tangential direction.

In this subsection, we will restrict ourselves to the simplest model of an adhesive tangential contact problem, with a conveniently defined "adhesion" in the normal direction and "friction" in the horizontal direction. This problem can be considered a generalization of the theory of Cattaneo and Mindlin to include adhesive contacts. We assume that the adhesive forces have sufficient range to be considered "macroscopic" with regards to the friction forces in the contact. In other words, we operate under the assumption that the adhesive forces create additional macroscopic pressure in the contact which, according to Coulomb's law of friction, leads to increased friction forces. Since both the normal and the tangential contact problem of two elastic bodies can be reduced to the contact between a rigid body and an elastic half-space (with modified material properties), we will consider—without loss of generality—the case of a rigid indenter in contact with an elastic half-space.

For the adhesive forces, we use the model of Dugdale where the adhesive pressure remains constant up to a certain distance h between the surfaces and abruptly drops to zero after that distance (3.147). The theory of adhesive contacts for this particular interaction was created by Maugis and is featured in Sect. 3.8 of this book. Therefore, the following theory can also be viewed as a generalization of the theory by Maugis relating to adhesive tangential contacts.

Let us consider a rigid indenter with a three-dimensional axially symmetric profile $f(r)$ and the corresponding MDR transformed profile $g(x)$. The profile $g(x)$ is initially pressed into the Winkler foundation, which are defined by the MDR rules, by d and subsequently displaced by $u^{(0)}$ in the tangential direction. The corresponding adhesive normal contact problem was solved in Sect. 3.8, from which the entire notation is inherited. For a sufficiently small rigid body displacement, the springs near the edge of the contact (contact radius a) slip while the springs in the interior zone (with the radius c) remain sticking. The radius c of the stick zone is given by the equation:

$$G^* u^{(0)} = \mu \left(2\sigma_0 \sqrt{b^2 - c^2} + E^* \left[d - g(c) \right] \right), \tag{4.121}$$

which sets the tangential force at the position c equal to the product of the normal force and the coefficient of friction. The total tangential force is calculated by integrating over all springs in the contact:

$$\begin{aligned} F_x &= 2\int_0^c G^* u^{(0)} \mathrm{d}x + 2\mu \int_c^a q_z(x)\mathrm{d}x \\ &= 2G^* u^{(0)} c + 2\mu \int_c^a \left(2\sigma_0\sqrt{b^2-x^2} + E^*[d-g(x)]\right)\mathrm{d}x \\ &= 2G^* u^{(0)} c + 2\mu\sigma_0 \left[x\sqrt{b^2-x^2} + b^2 \arcsin\frac{x}{b}\right]\Big|_c^a \\ &\quad + 2\mu E^* d(a-c) - 2\mu E^* \int_c^a g(x)\mathrm{d}x. \end{aligned} \tag{4.122}$$

The first term to the right-hand side is the contribution of the inner stick zone (rigid translation $u^{(0)}$). The second term is a contribution from springs in the slip zone (distributed load in the normal direction consisting of the elastic component $E^*[d-g(x)]$ and adhesive component $2\sigma_0\sqrt{b^2-x^2}$ given by (3.148), and multiplied with the coefficient of friction). Radius b of the interaction zone is determined from the equations of the normal contact problem which are listed in Sect. 3.8.

A complete theory of the tangential contact problem under those assumptions can be found in (Popov and Dimaki 2016). Here our consideration only deals with the limiting case of very short-range adhesive interactions (i.e., the parameter h is much smaller than all other characteristic system measures). This limiting case corresponds to the JKR approximation for the adhesive normal contact. The difference between the contact radius a and the radius of the adhesive interaction $b > a$ should, therefore, remain small:

$$\varepsilon = b - a \ll a, b. \tag{4.123}$$

In this approximation (see (3.160)),

$$\varepsilon = \frac{\pi h E^*}{4\sigma_0}. \tag{4.124}$$

For the normal contact problem, expanding by the small parameter ε yields (see (3.161)):

$$\begin{aligned} d &\approx g(a) - \sqrt{\frac{2\pi a \Delta\gamma}{E^*}}, \\ F_{N,\mathrm{JKR}}(a) &\approx 2E^* \int_0^a [d-g(x)]\mathrm{d}x, \end{aligned} \tag{4.125}$$

with

$$\Delta\gamma = \sigma_0 h, \tag{4.126}$$

which represent the exact JKR solution for an arbitrary axially symmetric profile.

Substituting $b = a + \varepsilon$ with ε from (4.124) into (4.121), and expanding to the lowest order of ε gives:

$$\frac{G^* u^{(0)}}{\mu} = \sqrt{4\sigma_0^2(a^2 - c^2) + 2\pi a E^* \Delta\gamma} - \sqrt{2\pi a E^* \Delta\gamma} + E^*[g(a) - g(c)]. \tag{4.127}$$

This equation determines the relationship between the radius of the stick zone c and the tangential body displacement $u^{(0)}$. It shows that even arbitrarily small tangential displacements induce partial slip in a narrow peripheral zone. This is in complete analogy to the case of the non-adhesive contact. The critical tangential displacement for the transition from partial to complete slip is calculated by setting $c = 0$:

$$\begin{aligned} u_c^{(0)} &= \frac{\mu}{G^*}\left(\sqrt{4\sigma_0^2 a^2 + 2\pi a E^* \Delta\gamma} + E^* g(a) - \sqrt{2\pi a E^* \Delta\gamma}\right) \\ &= \mu\left(\frac{1}{G^*}\sqrt{4\sigma_0^2 a^2 + 2\pi a E^* \Delta\gamma} + \frac{E^*}{G^*} d\right) \approx \mu\left(\frac{2\sigma_0}{G^*} a + \frac{E^*}{G^*} d\right). \end{aligned} \tag{4.128}$$

The approximation yields the tangential force:

$$\begin{aligned} \frac{F_x}{\mu} &= c\sqrt{4\sigma_0^2\,(a^2 - c^2) + 2\pi a E^* \Delta\gamma} - a\sqrt{2\pi a E^* \Delta\gamma} \\ &\quad + 2E^*[a g(a) - c g(c)] \\ &\quad + \pi\sigma_0 a^2\left(1 - \frac{2}{\pi}\arcsin\frac{c}{a}\right) - 2E^* \int_c^a g(x)\mathrm{d}x. \end{aligned} \tag{4.129}$$

At the onset of complete slip ($c = 0$) it is:

$$\begin{aligned} \frac{F_x}{\mu} &= \pi\sigma_0 a^2 + 2E^* a g(a) - a\sqrt{2\pi a E^* \Delta\gamma} - 2E^* \int_0^a g(x)\mathrm{d}x \\ &= \sigma_0 \pi a^2 + 2E^* \int_0^a [d - g(x)]\,\mathrm{d}x = \pi a^2 \sigma_0 + F_{N,\mathrm{JKR}}(a), \end{aligned} \tag{4.130}$$

where $F_{N,\mathrm{JKR}}(a)$ represents the solution of the adhesive normal contact problem in JKR approximation.

The final (4.130) could be written directly without the preceding calculations since the expression in parentheses ($\pi a^2 \sigma_0 + F_{N,\mathrm{JKR}}(a)$) is simply the total compressive force in the contact (sum of the elastic force and the additional adhesive

compressive force). According to Coulomb's law of friction, the tangential force for complete slip is equal to the total compressive force of the contacting surfaces multiplied with the coefficient of friction (independent of the particular pressure distribution in the contact).

4.7.1 The Paraboloid

A parabolic profile $\tilde{z} = f(r) = r^2/(2R)$ implies $g(x) = x^2/R$, and (4.127) and (4.129) take on the following form:

$$\begin{aligned}\frac{G^* u^{(0)}}{\mu} &= \sqrt{4\sigma_0^2(a^2-c^2) + 2\pi a E^* \Delta\gamma} - \sqrt{2\pi a E^* \Delta\gamma} \\ &\quad + \frac{E^*}{R}(a^2-c^2), \\ \frac{F_x}{\mu} &= c\sqrt{4\sigma_0^2(a^2-c^2) + 2\pi a E^* \Delta\gamma} - a\sqrt{2\pi a E^* \Delta\gamma} \\ &\quad + \pi\sigma_0 a^2\left(1 - \frac{2}{\pi}\arcsin\frac{c}{a}\right) + \frac{4}{3}\frac{E^*}{R}\left(a^3 - c^3\right). \end{aligned} \tag{4.131}$$

References

Cattaneo, C.: Sul Contatto di due Corpore Elastici: Distribuzione degli sforzi. Rendiconti Dell' Acad. Nazionale Dei Lincei **27**, 342–348, 434–436, 474–478 (1938)

Cerruti, V.: Ricerche intorno all' equilibrio de' corpi elastici isotropi. Memorie Dell'accademia Nazionale Dei Lincei **13**(3), 81–122 (1882)

Ciavarella, M.: Tangential loading of general three-dimensional contacts. J. Appl. Mech. **65**(4), 998–1003 (1998)

Ciavarella, M.: Indentation by nominally flat or conical indenters with rounded corners. Int. J. Solids Struct. **36**(27), 4149–4181 (1999)

Hamilton, G.M., Goodman, L.E.: The stress field created by a circular sliding contact. J. Appl. Mech. **33**(2), 371–376 (1966)

Hertz, H.: Über die Berührung fester elastischer Körper. J. Reine Angew. Math. **92**, 156–171 (1882)

Jäger, J.: Elastic contact of equal spheres under oblique forces. Arch. Appl. Mech. **63**(6), 402–412 (1993)

Jäger, J.: A new principle in contact mechanics. J. Tribol. **120**(4), 677–684 (1998)

Johnson, K.L.: Surface interaction between elastically loaded bodies under tangential forces. Proc. R. Soc. London Ser. A **230**, 531–549 (1955)

Johnson, K.L.: Contact mechanics. Cambridge University Press, Cambridge (1985)

Landau, L.D., Lifshitz, E.M.: Elastizitätstheorie. Lehrbuch der theoretischen Physik, vol. 7. Akademie Verlag, Berlin (1991)

Mindlin, R.D.: Compliance of elastic bodies in contact. J. Appl. Mech. **16**, 259–268 (1949)

Mindlin, R.D., Deresiewicz, H.: Elastic spheres in contact under varying oblique forces. J. Appl. Mech. **20**, 327–344 (1953)

Popov, V.L., Dimaki, A.V.: Friction in an adhesive tangential contact in the Coulomb-Dugdale approximation. J. Adhes. **93**(14), 1131–1145 (2017)

Popov, V.L., Heß, M.: Method of dimensionality reduction in contact mechanics and friction. Springer, Heidelberg (2015). ISBN 978-3-642-53875-9
Truman, C.E., Sackfield, A., Hills, D.A.: Contact mechanics of wedge and cone indenters. Int. J. Mech. Sci. **37**(3), 261–275 (1995)
Vermeulen, P.J., Johnson, K.L.: Contact of Non-spherical Elastic Bodies Transmitting Tangential Forces. J. Appl. Mech. **31**(2), 338–340 (1964)